JBC Papers in Press. Published on July 5, 2016 as Manuscript M116.739722
The latest version is at http://www.jbc.org/cgi/doi/10.1074/jbc.M116.739722

Thromboxane A2 activates YAP/TAZ to induce vascular smooth muscle cell proliferation and migration

Xu Feng[1], Peng Liu[1], Xin Zhou[1], Meng-Tian Li[1], Fu-Long Li[1], Zhen Wang[1], Zhi-Peng Meng[2], Yi-Ping Sun[1], Ying Yu[3], Yue Xiong[1,4*], Hai-Xin Yuan[1*] and Kun-Liang Guan[1,2*]

[1]Key Laboratory of Molecular Medicine of Ministry of Education and Institutes of Biomedical Sciences, Shanghai Medical College, Fudan University, Shanghai 200032, China
[2]Department of Pharmacology and Moores Cancer Center, University of California, San Diego, La Jolla, CA 92130, USA
[3]Key Laboratory of Food Safety Research, CAS Center for Excellence in Molecular Cell Science, Institute for Nutritional Sciences, Shanghai Institutes for Biological Sciences, Chinese Academy of Sciences, Shanghai 200031, China
[4]Department of Biochemistry and Biophysics, Lineberger Comprehensive Cancer Center, University of North Carolina at Chapel Hill, Chapel Hill, North Carolina, USA.

Correspondence to：
Yue Xiong, yxiong@email.unc.edu; Hai-Xin Yuan, yuanhaixin@fudan.edu.cn; Kun-Liang Guan, kuguan@ucsd.edu.

Running title: YAP/TAZ mediates Thromboxane A2 signaling
Keywords: Thromboxane A2; YAP/TAZ; Hippo; GPCR; vascular smooth muscle cells

ABSTRACT

Thromboxane A2 receptor (TP) has been implicated in restenosis after vascular injury, which induces vascular smooth muscle cell (VSMC) migration and proliferation. However, the mechanism for this process is largely unknown. In the current study, we reported that TP signaling induces VSMC migration and proliferation through activating YAP/TAZ, two major downstream effectors of the Hippo signaling pathway. The TP specific agonists I-BOP and U-46619 induce YAP/TAZ activation in multiple cell lines, including VSMCs. YAP/TAZ activation induced by I-BOP is blocked by knockout of the receptor *TP* or knockdown of downstream G-proteins $G\alpha_{12/13}$. Moreover, Rho inhibition or actin cytoskeleton disruption prevents I-BOP induced YAP/TAZ activation. Importantly, TP activation promotes DNA synthesis and cell migration in VSMCs in a manner dependent on YAP/TAZ. Taken together, Thromboxane A2 signaling activates YAP/TAZ to promote VSMCs migration and proliferation, indicating YAP/TAZ as potential therapeutic targets for cardiovascular diseases.

Thromboxane A2 (TxA2) is produced in many cells/tissues, particularly in the platelet (1), and plays an important role in platelet activation and aggregation in vascular injury and atherosclerosis (2). In patients with atherosclerosis or undergoing percutaneous transluminal coronary angioplasty (a non-surgical procedure used to treat the narrowed coronary arteries in cardiovascular disease), the concentration of TxA2 is significantly increased (3-5). Similar phenomenon has also observed in the corresponding mouse models (6-8). TxA2 and Thromboxane A2 receptor (TP) are believed to

contribute to restenosis after vascular injury (6,9), which remains a challenging clinical problem, although drug-eluting stents can reduce the risk of restenosis (10).

TxA2 is a type of prostanoids, a family of lipid mediators generated by cyclooxygenase. TxA2 is unstable with a half-life of about 30 seconds and is non-enzymatically degraded into biologically inactive form thromboxane B2 (TxB2) (1). TxA2 exerts its biological activity through its cognate TP receptor, a G protein-coupled receptor (GPCR) that couples with $G\alpha_{12/13}$, $G\alpha_{q/11}$ and other trimeric G proteins to regulate downstream effectors (11). TP is expressed as two isoforms in human, TPα and TPβ respectively. Besides TxA2, prostaglandin H2, isoprostanes (such as 8-iso-$PGF_{2\alpha}$), and hydroxyeicosatetraenoic acids can also activate the TP receptors (12-14).

In addition to platelet activation, TxA2 or TP receptor is also known to promote cell migration and proliferation of vascular smooth muscle cells (VSMCs) (15-20), an important process that is involved in a number of vascular diseases, such as post-angioplasty restenosis and atherosclerosis (21). The proliferative response of VSMCs to vascular injury is markedly exaggerated in the transgenic mice with vascular overexpression of the human TPα receptor, which can be inhibited by TP specific antagonist S18886 (6). Moreover, the injury-induced vascular proliferation and platelet activation are suppressed in mice genetically deficient in TP receptor (6). In mouse models of atherosclerosis, both pharmacological antagonism and TP receptor deletion delay lesion development (22-24). Taken together, these previous studies demonstrate that TxA2 and TP receptor contribute to VSMCs mediating vascular disease, although the molecular mechanism is largely unknown.

The Hippo signaling pathway plays a key role in the regulation of organ size and tissue homeostasis (25). Core components of the mammalian Hippo pathway include MST1/2 and their adaptor protein SAV1, LATS1/2 and their adaptor proteins MOB1A/1B, and two downstream transcriptional effectors YAP/TAZ (25). MST1/2 phosphorylate and activate LATS1/2 kinases, which in turn phosphorylate and inhibit YAP/TAZ. Recently MAP4Ks have been shown as core components of the Hippo pathway, and function in parallel to MST1/2 to phosphorylate and activate LATS1/2 (26,27). Phosphorylation of YAP at S127 results in cytoplasmic sequestration due to 14-3-3 binding (28,29). The dephosphorylated YAP/TAZ translocate into the nucleus and interact with the TEAD family transcription factors to induce target genes, such as connective tissue growth factor (CTGF) and cysteine-rich angiogenic inducer 61 (CYR61), thereby promoting cell proliferation, migration and survival (30-32). Deregulation of the Hippo pathway has been observed in various human cancers, and is often correlated with poor prognosis (33). Upstream signals of the Hippo pathway had been elusive until recently, studies have established that GPCRs relay extracellular signals to the Hippo pathway (34-38). Ligands signal through GPCRs coupled to $G\alpha_{12/13}$, $G\alpha_{q/11}$ or $G\alpha_{i/o}$ activate YAP/TAZ, whereas ligands signal through $G\alpha_s$-coupled GPCRs suppress YAP/TAZ activity (36). Therefore, stimulation of different GPCRs can result in either activation or inhibition of YAP/TAZ.

Interestingly, emerging evidence shows that YAP is induced after arterial injury, and its activation promotes smooth muscle phenotypic switch and neointima formation (39,40). This led us to investigate the fucntion of YAP/TAZ in TxA2- and TP receptor-induced cellular signaling, VSMCs migration and proliferation. In the present study, we show that TP activation increases YAP/TAZ activity in VSMCs and other cell types via $G\alpha_{12/13}$. Importantly, YAP/TAZ are essential for TP-induced VSMC proliferation and migration, thus provides a

plausible mechanism for VSMC mediated vascular diseases.

RESULTS

Stimulation of TP induces YAP/TAZ dephosphorylation and nuclear accumulation

To study TP regulation on YAP/TAZ activity, we treated cells with TP agonist I-BOP because the physiological TP ligand TxA2 is extremely unstable. In serum-starved HeLa cells that express TP, YAP was highly phosphorylated. Addition of I-BOP resulted in a significant decrease in YAP phosphorylation, as determined by immunoblotting with a phospho-YAP antibody (S127) (Figure 1A, B). I-BOP also induced TAZ dephosphorylation as indicated by the differential migration on phos-tag gels (Figure 1B). Moreover, I-BOP-induced YAP/TAZ dephosphorylation was rapid and transient, as the YAP/TAZ dephosphorylation was visible 15 minutes upon stimulation and partially recovered 4 h after I-BOP treatment (Figure 1B). In addition, U-46619, another TP specific agonist, could also induce YAP/TAZ dephosphorylation in a dose- and time-dependent manner (Supplemental Figure 1A, B).

Phosphorylation of YAP at S127 by LATS1/2 leads to binding with 14-3-3 and cytoplasmic sequestration of YAP, and dephosphorylated YAP accumulates in the nucleus and induces gene expression by interacting with transcription factors TEAD1-4 (29,31). Similarly, phosphorylation of TAZ at S89 by LATS1/2 also induces cytoplasmic localization(30). As expected, I-BOP treatment caused significant nuclear accumulation of YAP and TAZ (Figure 1C, D; Supplemental Figure 1C), and enhanced the interaction between YAP and TEAD1 (Figure 1E). Similar effect was also observed when cells were treated with U-46619 (Figure 1C, D; Supplemental Figure 1C). To confirm the functional activation of YAP/TAZ upon TP stimulation, we examined the expression of well-established YAP/TAZ target genes. The mRNA levels of CTGF and CYR61 were significantly induced by I-BOP or U-46619 treatment (Supplemental Figure 1D, E). Accordingly, CYR61 protein level was also increased upon I-BOP stimulation (Figure 1B).

The effect of TP activation on YAP/TAZ was consistently observed in multiple cell lines, including MDA-MB-231, SW480, and HEK293A (Supplemental Figure 1F-1I). Notably, I-BOP also induces YAP/TAZ dephosphorylation in VSMCs, such as T/G HA-VSMC cell line and primary mouse aortic VSMC (MAVSMC) (Figure 1F-H). The effect of I-BOP on YAP/TAZ phosphorylation was dose dependent, and YAP/TAZ dephosphorylation was evident when as low as 0.1 nmol/L I-BOP was added to primary MAVSMCs (Figure 1H). Similarly, the expression of YAP/TAZ target genes, such as CTGF, CYR61, TAGLN and EDN1, were significantly induced by I-BOP in T/G HA-VSMCs (Figure 1I). Based on the above data, we conclude that stimulation of TP activates YAP/TAZ by inducing their dephosphorylation and nuclear translocation.

I-BOP acts through TP and $G\alpha_{12/13}$ to activate YAP/TAZ

Due to the unstable property of TxA2, I-BOP and U-46619 were used to treat cells. To exclude that these chemicals have unexpected effect on YAP/TAZ independent of TP, we pretreated cells with TP specific antagonist SQ-29548 followed by I-BOP treatment. As shown in Figure 2A, the I-BOP-induced YAP/TAZ dephosphorylation was blocked by SQ-29548 in T/G HA-VSMCs. HEK293A cells are not very sensitive to I-BOP stimulation, likely due to low level of TP expression. Ectopic expression of TPα receptor rendered YAP/TAZ more sensitive to 1 nmol/L I-BOP treatment, a concentration that had a minor effect on YAP/TAZ phosphorylation in the control

HEK293A cells (Figure 2B). Similar phenomenon was observed when TPβ was overexpressed in U2OS cells (Supplemental Figure 2). These data indicate that I-BOP acts through both isoforms of TP receptor to activate YAP/TAZ.

To further confirm the role of endogenous TP in YAP/TAZ regulation, we generated *TP* knockout (*TP*-KO) cells using the CRISPR/Cas9 genome-editing system. Two independent *TP*-KO cell lines were generated and the TP deletion was verified by Sanger sequencing (Supplemental Figure 3). *TP* knockout completely blocked I-BOP-induced YAP/TAZ dephosphorylation and YAP nuclear accumulation (Figure 2C, D). Consistently, I-BOP was unable to induce the expression of YAP target genes in *TP*-KO cells (Figure 2E). These data show that I-BOP stimulates TP receptor to induce YAP/TAZ activation.

TP receptor activates several trimeric Gα proteins, including $G\alpha_{q/11}$ and $G\alpha_{12/13}$, to initiate intracellular signaling pathways (11). To determine which Gα proteins are involved in YAP/TAZ regulation, $G\alpha_{q/11}$ or $G\alpha_{12/13}$ were knocked down by RNAi in HEK293A cells (Figure 2F). Knockdown of $G\alpha_{12/13}$ strongly blocked YAP/TAZ dephosphorylation in response to I-BOP, while knockdown of $G\alpha_{q/11}$ had little effect on I-BOP-induced YAP/TAZ dephosphorylation (Figure 2F). Consistently, I-BOP induced YAP nuclear accumulation in control siRNA- and $G\alpha_{q/11}$ siRNA-transfected cells, but not in $G\alpha_{12/13}$ siRNA-transfected cells (Figure 2G; Supplemental Figure 4). Taken together, we conclude that TP signals through $G\alpha_{12/13}$ to induce YAP/TAZ dephosphorylation and activation.

I-BOP modulates YAP/TAZ dephosphorylation via Rho GTPase and actin cytoskeleton

Rho GTPase is a known downstream signaling module of $G\alpha_{12/13}$, which directly interacts and activates the Rho guanine nucleotide exchange factor. We therefore tested the role of Rho GTPase in I-BOP-induced YAP/TAZ dephosphorylation. Expression of Rho GDP dissociation inhibitor (Rho-GDI), which binds to Rho GTPase and inhibits GTPase cycling, suppressed I-BOP-induced YAP/TAZ dephosphorylation (Figure 3A). Likewise, *botulinum* toxin C3, a specific inhibitor of Rho GTPase, strongly blocked YAP/TAZ dephosphorylation in response to I-BOP or U-46619 treatment (Figure 3B; Supplemental Figure 5A and 5B). Consistently, C3 treatment blocked the I-BOP- or U-46619-induced YAP nuclear translocation (Figure 3C; Supplemental Figure 5C). These data indicate that Rho GTPase is required for TP to activate YAP/TAZ.

The major function of Rho GTPase is to modulate actin cytoskeleton, particularly stress fiber formation. Recently studies have shown that actin cytoskeleton plays an important role in the Hippo pathway (41-45). We therefore tested whether cytoskeletal reorganization contributes to YAP/TAZ activation by TP agonists. Latrunculin B (LatB), a F-actin-disrupting reagent, blocked I-BOP- or U-46619-induced YAP/TAZ dephosphorylation (Figure 3D; Supplemental Figure 5D). Consistent with changes in YAP phosphorylation, LatB treatment also prevented YAP nuclear accumulation in response to I-BOP or U-46619 (Figure 3E; Supplemental Figure 5E). Moreover, I-BOP or U-46619 induced actin stress fiber and YAP nuclear translocation (Figure 2G, 3C and 3E; Supplemental Figure 5C and 5E). Knockdown of $G\alpha_{12/13}$ or treatment with C3 or LatB disrupted F-actin formation and YAP nuclear accumulation (Figure 2G, 3C and 3E; Supplemental Figure 5C and 5E). These results indicate TP acts through Rho GTPase and actin cytoskeleton to affect YAP/TAZ phosphorylation.

I-BOP inhibits LATS

LATS1/2 are the kinases directly responsible for YAP/TAZ phosphorylation. The phosphorylation of activation loop (S909/S872 for LATS1/2) and hydrophobic motif (T1079/T1041 for LATS1/2) correlates with LATS1/2 kinase activity (46). To test whether LATS1/2 kinases are involved in I-BOP induced YAP/TAZ activation, we measured LATS1 kinase activity *in vitro*. LATS1 was potently inhibited by I-BOP treatment, as determined by its auto-phosphorylation at S909 and the *in vitro* phosphorylation of the purified GST-YAP (Figure 4A). Consistent with the results described in Figure 3B and 3C, inhibition of Rho GTPase by C3 blocked the inhibitory effect of I-BOP on LATS1 kinase activity (Figure 4A), indicating that Rho GTPase activation is required for I-BOP-induced LATS1 inhibition. To further determine the role of LATS1/2 in YAP regulation by I-BOP, we used *LATS1/2* double knockout (LATS1/2-dKO) HEK293A cells. As expected, I-BOP could not affect YAP/TAZ phosphorylation in LATS1/2-dKO cells (Supplemental Figure 6), suggesting that LATS1/2 are required for I-BOP-induced YAP/TAZ dephosphorylation.

MST1/2 and MAP4Ks are responsible for LATS kinases activation in response to upstream signals(26,27,46). To test whether MST1/2 or MAP4Ks are involved in I-BOP-induced YAP/TAZ dephosphorylation, we used *MST1/2* double knockout (MST1/2-dKO) and combined deletion of *MST1/2* and *MAP4K1/2/3/4/5/6/7* (MM-9KO) HEK293A cells (Supplemental Figure 7). I-BOP-induced YAP/TAZ dephosphorylation was largely unaffected in MST1/2-dKO cells (Figure 4B). However, I-BOP had no effect on YAP/TAZ phosphorylation in MM-9KO cells (Figure 4C). In addition, re-expression of MST2 or MAP4K2 could restore I-BOP's effect on YAP phosphorylation in MM-9KO cells (Figure 4D). I-BOP-induced LATS inhibition was abolished in MM-9KO cells as shown by *in vitro* kinase assay (Figure 4E). Taken together, these results suggest that MAP4Ks play a major role in I-BOP-induced YAP/TAZ dephosphorylation, though both MST1/2 and MAP4Ks are involved.

YAP/TAZ are required for TP to stimulate VSMC DNA synthesis and cell migration.

TP has been shown to promote neointima formation, which is caused by VSMC migration and proliferation (6,9,47). Since YAP/TAZ activity is significantly activated upon TP stimulation in VSMCs, we investigated whether YAP/TAZ activation is involved in the proliferation and migration of VSMCs. *YAP/TAZ* were knocked down in T/G HA-VSMC by inducible shRNA and siRNA respectively. The knockdown efficiency was confirmed by immunoblotting of protein levels (Figure 5A). Knockdown of *YAP/TAZ* significantly suppressed the mRNA induction of CTGF and CYR61 in response to I-BOP (Figure 5B). I-BOP strongly induced cell migration in control cells, while this effect was significantly suppressed in *YAP/TAZ* double knockdown cells (Figure 5C and 5D). In addition, I-BOP-induced VSMC DNA synthesis was also suppressed by *YAP/TAZ* double knockdown as determined by EdU incorporation (Figure 5E; Supplemental Figure 8A). To further support the important role of TP-YAP/TAZ axis in VSMCs , we isolated and analyzed primary MAVSMCs. Similar *Yap*/*Taz* knockdown experiments were performed in primary MAVSMCs. Consistently, knockdown of *Yap/Taz* in primary MAVSMCs also inhibited cell migration induced by I-BOP (Figure 5F-5H). In addition, we observed that YAP/TAZ knockdown suppressed I-BOP-induced gene expression and cell migration in HeLa cells (Supplemental Figure 8B-8D). Taken together, these results demonstrate that YAP/TAZ play an important role in TP-mediated gene induction, cell

proliferation and migration in VSMCs.

DISCUSSION

TxA2 is involved in multiple physiological and pathophysiological processes, including thrombosis, asthma, myocardial infarction, inflammation, atherosclerosis and the response to vascular injury (11). TxA2 exerts its biological activity via its cognate TP receptor. In this study, we demonstrate that the Hippo pathway is a crucial downstream signaling module of TP receptor, a classical GPCR. TP agonists significantly activate YAP/TAZ in multiple cells lines, including vascular smooth muscle cells (VSMCs). Our data also demonstrate that activation of TP couples to $G\alpha_{12/13}$ to trigger the activation of Rho GTPase, which modulates actin cytoskeleton to inhibit LATS1/2 kinase activity, resulting in YAP/TAZ dephosphorylation and activation (Figure 6). In this signaling cascade, both MST1/2 and MAP4Ks, the major kinases for LATS1/2, are involved in the Hippo pathway regulation by TP. Our studies indicate a functional role of the Hippo pathway and YAP/TAZ in mediating the physiological and pathological functions of thromboxane and its receptor TP.

In addition to TxA2, there are four other major prostaglandins generated from arachidonic acid *in vivo*, including prostaglandin D_2 (PGD_2), prostaglandin E_2 (PGE_2), prostaglandin $F_{2\alpha}$ ($PGF_{2\alpha}$), and prostacyclin (PGI_2) (48). They all exert their effects via corresponding GPCRs. It is interesting to speculate that YAP/TAZ may play a similar role in physiological and disease processes that are regulated by prostaglandins, such as inflammation, atherosclerosis, and cancer (49). For instance, the prostacyclin receptor (IP) couples to $G\alpha_s$ and stimulates cAMP production and PKA activation(50). Previously we reported that cAMP acts through PKA to stimulate LATS kinases and inhibit YAP (51). Given that TxA2 and PGI_2 are antagonistic in their actions in cardiovascular disease(6), it will be interesting to determine whether PGI_2 inhibits YAP/TAZ, thereby antagonizing the effect of TxA2, which activates YAP/TAZ as shown in this report, in cardiovascular disease.

Isoprostanes are free-radical-catalyzed peroxidation of unsaturated fatty acids, such as arachidonic acid, which are recognized not only as reliable markers of oxidative stress but also as important mediators of various diseases (52). Increased formation of isoprostanes has been observed in diseases that are linked to oxidative stress, such as cardiovascular disease and cancer (52). As mentioned above, isoprostanes act, at least partially, via TP to exert their physiological effects. So one may speculate that YAP/TAZ also play a role in isoprostanes mediated pathophysiological effects. Indeed, we observed that 8-iso-PGF2a, a type of isoprostanes, could induce YAP/TAZ dephosphorylation in VSMCs (unpublished data). Future studies are needed to delineate the involvement and potential role of YAP/TAZ in isoprostanes-induced physiological processes.

Our study shows that YAP/TAZ are required for TP-stimulated VSMC DNA synthesis and cell migration. The connection between TP receptor and the Hippo pathway in vascular smooth muscle cells has important physiological implications. During vascular injury, activated platelets or other cells produce TxA2, which in turn promotes platelet activation and aggregation (4,53). Besides TxA2, isoprostanes may also act through the TP receptor on the surface of smooth muscle cell and initiate the migration from media to intima via YAP/TAZ activation. Previous studies have reported YAP is activated in VSMCs of neointima (39). We propose that thromboxane acts through TP to induce YAP/TAZ activation to promote normal physiological wound healing in response to vascular injury. However, too much YAP/TAZ activation by TP under pathological conditions may lead to VSMC

overgrowth, thereby contributing to neointima formation and restenosis. Notably, the CTGF and CYR61 are strongly induced upon TP stimulation in a manner dependent on YAP/TAZ (Figure 2E, 5B). Both CTGF and CYR61 have been shown to promote atherosclerotic lesions development and neointimal hyperplasia (54-56), therefore, uncontrolled expression of these proteins may contribute to pathology associated with TP hyperactivation. No TP antagonist has been used in clinics, due to efficacy and toxicity issues (2). Our work reveals new insights of the role of the Hippo pathway and YAP/TAZ in thromboxane pathophysiology and suggests that YAP/TAZ as potential therapeutic targets for vascular diseases. Actually a small molecule verteporfin (trade name Visudyne), a clinical drug for neovascular macular degeneration (57), has been shown to efficiently inhibit TEAD-YAP interaction and suppress YAP-induced liver overgrowth (58). The data in this report suggests that YAP/TAZ inhibitors could be a potential treatment of vascular diseases caused by VSMC overgrowth.

EXPERIMENTAL PROCEDURES

Plasmids

The plasmids of pCMV-HA-YAP2, Flag-LATS1, Flag-MST2, Flag-MAP4K2 and GFP-GDI were described before(26,51,59). TPα/β were amplified from cDNA then subcloned into pRK7-N-Flag and pQCXIH vectors with restriction enzymes BamHI/EcoRI.

Antibodies

Antibodies for YAP (#4912), Phospho-YAP(S127) (#4911), MST1 (#3682), MST2 (#3952), CYR61 (#11952), Phospho-MST1(T183)/MST2(T180) (#3681), Phospho-LATS1(S909) (#9157) and Phospho-LATS1 (T1079) (#8654) were purchased from Cell Signaling Technology. The LATS1 (A300-477A) and YAP (A302-308A) antibodies used for Immunoprecipitation and LATS2 (A300-479A) antibody were from Bethyl Laboratories. TAZ (HPA007415) and Vinculin (#V9264) antibodies were obtained from Sigma-Aldrich. Anti-TEAD1 (610922) was purchased from BD Transduction Laboratories. Antibodies for $G\alpha_{q/11}$ antibody (C-19) (sc-392), $G\alpha_{12}$ antibody (S-20) (sc-409) and HA-probe antibody (sc-7392) were from Santa Cruz Biotechnology. Tubulin antibody (#581P) were purchased from NeoMarkers, Anti-β-actin (A00702), Lamin A/C (A01455) and anti-Flag antibodies were purchased from GeneScript. GFP-Tag (7G9) (#M20004) were from Abmart. Anti-G protein alpha 13 antibody [EPR5436] (ab128900) was obtained from Abcam.

Chemicals

U-46619 (9,11-dideoxy-9α,11α-methanoepoxy-prosta-5Z,13E-dien-1-oic acid) and SQ-29548 ([1S-[1α,2α(Z),3α,4α]]-7-[3-[[2-[(phenylamino) carbonyl]hydrazino]methyl]-7-oxabicyclo[2.2.1] hept-2-yl]-5-heptenoic acid) were purchased from Santa Cruz. I-BOP ([1S-[1α,2α(Z),3β(1E,3S*),4 α]]-7-[3-[3-hydroxy-4-(4-iodophenoxy)-1-butenyl]-7-oxabicyclo[2.2.1]hept-2-yl]-5-heptenoic acid) was purchased from Cayman Chemical. Latrunculin B and Tetramethylrhodamine B isothiocyanate-conjugated Phalloidin were purchased from Sigma-Aldrich. C3 was from Cytoskeleton Inc. Phos-tag was purchased from Wako chemicals. DAPI was purchased from Invitrogen.

Generation of knockout cells using CRISPR/Cas9 genome editing

To generate TP knockout HEK 293A cells, the guide sequence targeting the human *TBXA2R* gene was used: 5′-GCTGGTGACCGGTACCATCG-3′. The detail protocol was described elsewhere(26). Two independent clones with *TBXA2R* gene deletion were used for experiments. MST1/2-dKO and LATS1/2-dKO HEK293A

cells were described previously(26). MM-9KO HEK293A cells was generated based on MM-8KO cells (26). The guide sequences targeting the human *MAP4K5* gene were used: 5′-CACCTACGGGGACGTCTATA-3′. Gene deletion was verified by Sanger sequencing of genomic DNA (Supplemental Fig. S3, S7).

Cell culture

HEK239A and HeLa cells were cultured in DMEM medium (Invitrogen). U2OS cells were cultured in RPMI-1640 medium (Invitrogen). All of the above cells were supplemented with 10% fetal bovine serum (FBS) (Gibco) and 50 μg/ml penicillin/streptomycin (P/S). T/G HA-VSMCs were cultured in DMEM/F12 medium (Invitrogen) and supplemented with 0.05 mg/ml ascorbic acid, 0.01 mg/ml insulin, 0.01 mg/ml transferrin, 10 ng/ml sodium selenite, 0.03 mg/ml Endothelial Cell Growth Supplement (ECGS), and 50μg/ml P/S. Mouse primary aortic VSMC cells were isolated from 4-8 week-old C57BL/6 male mice using a standard protocol(60), and incubated in DMEM medium supplemented with 20% FBS, and 50μg/ml P/S. Cells at passage 3 to 5 were used. For serum starvation, cells were incubated in DMEM or DMEM/F12 without serum. All cell lines were maintained at 37°C with 5% CO2.

Transfection, lentiviral and retroviral infection

Cells were transfected with plasmid DNA using polyethylenimine (PEI). To generate U2OS cells stably expressing TPα/β, retroviruses carrying pQCXIH empty vector or pQCXIH-TPα/β were produced in HEK293T cells using VSVG and GAG as packaging plasmids. Virus supernatant was filtered through 0.45-μm filter and was used to infect targeting cells in the presence of 8 μg/ml polybrene. Stable cell pools were selected with 50μg/mL hygromycin B (Amresco) for 5 days. For tetracycline-inducible shRNA expression, lentivirus containning shRNAs in the pTRIPZ vector was made in HEK293T cells using pMD2.g and psPAX2 as packaging plasmids. Virus infection was performed as described above except selection with 1μg/mL puromycin (Amresco) for 5 days. Expression of shRNA was induced by adding 1μg/mL Doxycycline for 48h.

The shRNA sequence against YAP were shown below：

YAP#1: TTCTTTATCTAGCTTGGTGGC

YAP#2: TGGTCAGAGATACTTCTTAAA

RNA interference

siRNAs targeting *GNAQ, GNA11, GNA12, GNA13, YAP1/Yap1, WWTR1/Wwtr1* were from Genepharma and were delivered into cells using RNAiMAX (Invitrogen) according to the manufacturer's instructions. The sequences of all small interfering RNAs (siRNAs) used in this study were shown below:

si*GNAQ* #1: GACACCGAGAATATCCGCTTT

si*GNAQ* #2: CTATGATAGACGACGAGAATA

si*GNA11* #1: GCTCAAGATCCTCTACAAGTA

si*GNA11*#2: GCTCAACCTCAAGGAGTACAA

si*GNA12*#1: GCGACACCATCTTCGACAA

si*GNA12*#2: GGATGTTCCTGATGGCCTT

si*GNA13*#1: GCTCGAGAGAAGCTTCATA

si*GNA13*#2: CCTGCTATAAGAGCATTAT

si*YAP1*#1: CCCAGTTAAATGTTCACCAAT

si*YAP1*#2: CAGGTGATACTATCAACCAAA

si*TAZ*#1: CAGCCAAATCTCGTGATGAAT

si*TAZ*#2: GCGATGAATCAGCCTCTGAAT

si*Yap1*#1: GAAGCGCTGAGTTCCGAAATC

si*Yap1*#2: TGAGAACAATGACAACCAATA

si*Taz*#1: CAGCCGAATCTCGCAATGAAT

si*Taz*#2: CCATGAGCACAGATATGAGAT

RNA extraction and real-time PCR

Cells were washed with cold phosphate-buffered saline (PBS), and total RNA was isolated using Trizol reagent following the manufacturer's instruction (Invitrogen). 1μg RNA was reverse transcribed to complementary DNA (cDNA) with oligo-dT primers (Transgene). cDNA was then diluted and subjected to real-time PCR with gene-specific primers using SYBR Premix Ex Taq (TaKaRa) and the 7500 real-time PCR system (Applied Biosystems). The primer pairs

used in this study were:
Actin:
GCCGACAGGATGCAGAAGGAGATCA/AAGCATTTGCGGTGGACGATGGA
CTGF:
CCAATGACAACGCCTCCTG/TGGTGCAGCCAGAAAGCTC
CYR61:
AGCCTCGCATCCTATACAACC/TTCTTTCACAAGGCGGCACTC
EDN1:
TGTGTCTACTTCTGCCACCT/CCCTGAGTTCTTTTCCTGCTT
ANKRD1:
CACTTCTAGCCCACCCTGTGA/CCACAGGTTCCGTAATGATTT
TAGLN:
CCCGAGAACCCACCCTCCA/AAAGCCATCAGGGTCCTCTGC
TPα:
CCTTCTGGTCTTCATCGCCC/CTGGAGGGACAGCGACCT
TPβ:
ACCCGGCCCAGACGGAGT/GGACAGAGCCTTCCCTGTTGG

Immunoprecipitation (IP)

Cells were lysed using lysis buffer (50 mM Tris at pH 7.5, 150 mM NaCl, 0.5% NP-40, 50 mM NaF, 1.5 mM Na_3VO_4, 1 mM PMSF and protease inhibitors). Cell lysates were centrifuged at 12,000 × g for 15 min at 4°C. The supernatants were incubated with YAP antibody (Bethyl Laboratories) for 2 h, followed by protein A agarose beads incubation for 1 h. Immunoprecipitates were washed 3 times with lysis buffer, and proteins were boiled with SDS-PAGE sample buffer.

Immunoblotting

Cells were lysed in SDS sample buffer and denatured by heating on 99°C for 10 min. Immunoblotting was performed in 8% or 10% Bis-Tris polyacrylamide gel according to the standard protocol. The phos-tag reagents were purchased from Wako Chemicals, and gels containing phos-tag were prepared following the manufacturer's instructions. YAP and TAZ proteins can be separated into multiple bands in phos-tag gels depending on differential phosphorylation levels, with phosphorylated YAP/TAZ migrating more slowly.

Immunofluorescence staining

Cells seeded in 6-well plates were treated as indicated in specific experiments. After treatment, they were fixed immediately with 4% paraformaldehyde for 20 min and then permeabilized with 0.5% Triton X-100 in PBS for 5 min on ice. After blocking in 5% BSA for 30 min, cells were incubated with primary antibodies overnight at 4°C. Cells were washed with PBS 3 times for 5 min, and Alexa Fluor 488 conjugated secondary antibodies were added for 1 h at room temperature. Tetramethylrhodamine B isothiocyanate-conjugated Phalloidin was used to stain actin filaments, and DAPI was used for cell nuclei. Photos were taken by an Olympus IX81 Inverted Research Microscope with appropriate fluorescence filters.

Cell fractionation

HeLa cells were seeded with a density of 6×10^4 cells/cm^2 for 12 h then starved in serum-free medium for 16 h and stimulated with 1 nmol/L I-BOP or 10 nmol/L U-46619 for 1 h. Subcellular fractionation was performed with NE-PER™ Nuclear and Cytoplasmic Extraction Reagents (ThermoFisher) according to the manufacturer's instructions. Both fractions were analyzed by Western blot.

***In vitro* kinase assay**

LATS1 kinase assay was performed as described before(38). Briefly, LATS1 was immunoprecipitated from cells and subjected to an *in vitro* kinase assay using GST-YAP as a substrate. The phosphorylation levels of GST-YAP at Ser127 residue were determined by immunoblotting using Phospho-YAP (S127) antibody.

Transwell migration assay

Cell migration assays were performed using BD Falcon Cell culture inserts for 24-well plates with 8.0 μm pores filter. Cells were serum starved for 20 h and then stimulated with I-BOP or vehicle for 4 h. Cells (6×10^4 for T/G HA-VSMC, 5×10^4 for primary aortic VSMC, 2×10^5 for HeLa) were seeded into the upper chamber of the insert for each well in DMEM/F-12 without other supplements, and the lower chamber of the plate was filled with DMEM/F-12 supplemented with 10% FBS. After 6 h for T/G HA-VSMC (3 h for primary MAVSMC, 24 h for HeLa), cells were fixed using 4% paraformaldehyde and stained with 0.05% crystal violet. Cells in the upper chamber were removed by scrubbing with a cotton swab, and cells migrated through the filter were photographed and quantified.

EdU incorporation assay

T/G HA-VSMCs grown on 24-well plates were serum starved for 24 h. In the meantime, I-BOP (1 nmol/L) was added every 8 h for 3 times. 10 μmol/L EdU (5-Ethynyl-2'-Deoxyuridine) was added to the culture media for 4 h. After labeling, cells were fixed with 4% paraformaldehyde for 20 min followed by permeabilization with 0.5% Triton X-100 in PBS for 20 min at room temperature. Cells were rinsed once with PBS and incubated with the cocktail reaction buffer (100 mmol/L sodium ascorbate, 4.8 μmol/L Alexa Fluor 488 Azide, 4 mmol/L CuSO4) for 30 min at room temperature. After staining, cells were washed 3 times with 0.5% Triton X-100 in PBS, and DAPI was used for cell nuclei. Photos were taken by an Olympus IX81 Inverted Research Microscope.

Statistical Analysis

All data are expressed as mean ± SEM. Two groups comparison was analyzed by Student's *t* test. P Values < 0.05 were considered significant and labeled with one asterisk.

Acknowledgments: We thank Dan Ye and the members of Fudan MCB Lab for the supports throughout the course of this study.

Conflict of interest: K.L.G. is a cofounder of Vivace Therapeutics Inc.

Author contributions: X.F., Y.X., H.-X. Y and K.-L.G designed the research, analyzed the data, and wrote the manuscript; X.F. performed the experiments with the assistance from P.L., X.Z., M.-T. L, F.-L. L, Z.W., Z.M., Y.-P. S; Y.Y. provided technical and intellectual support; All authors discussed the results and commented on the manuscript.

REFERENCES

1. Hamberg, M., Svensson, J., and Samuelsson, B. (1975) Thromboxanes: a new group of biologically active compounds derived from prostaglandin endoperoxides. *Proc Natl Acad Sci U S A* **72**, 2994-2998
2. Ting, H. J., Murad, J. P., Espinosa, E. V., and Khasawneh, F. T. (2012) Thromboxane A2 receptor: biology and function of a peculiar receptor that remains resistant for therapeutic targeting. *Journal of cardiovascular pharmacology and therapeutics* **17**, 248-259
3. Braden, G. A., Knapp, H. R., and FitzGerald, G. A. (1991) Suppression of eicosanoid biosynthesis during coronary angioplasty by fish oil and aspirin. *Circulation* **84**, 679-685
4. Byrne, A., Moran, N., Maher, M., Walsh, N., Crean, P., and Fitzgerald, D. J. (1997) Continued thromboxane A2 formation despite administration of a platelet glycoprotein IIb/IIIa antagonist in patients undergoing coronary angioplasty. *Arteriosclerosis, thrombosis, and vascular biology* **17**, 3224-3229
5. Belton, O., Byrne, D., Kearney, D., Leahy, A., and Fitzgerald, D. J. (2000) Cyclooxygenase-1 and -2-dependent prostacyclin formation in patients with atherosclerosis. *Circulation* **102**, 840-845
6. Cheng, Y., Austin, S. C., Rocca, B., Koller, B. H., Coffman, T. M., Grosser, T., Lawson, J. A., and FitzGerald, G. A. (2002) Role of prostacyclin in the cardiovascular response to thromboxane A2. *Science* **296**, 539-541
7. Belton, O. A., Duffy, A., Toomey, S., and Fitzgerald, D. J. (2003) Cyclooxygenase isoforms and platelet vessel wall interactions in the apolipoprotein E knockout mouse model of atherosclerosis. *Circulation* **108**, 3017-3023
8. Pratico, D., Cyrus, T., Li, H., and FitzGerald, G. A. (2000) Endogenous biosynthesis of thromboxane and prostacyclin in 2 distinct murine models of atherosclerosis. *Blood* **96**, 3823-3826
9. Yamagami, S., Miyauchi, K., Kimura, T., Goh, Y., Daida, H., and Yamaguchi, H. (1999) Effects of the thromboxane A2 receptor antagonist on platelet deposition and intimal hyperplasia after balloon injury. *Japanese heart journal* **40**, 791-802
10. Inoue, T., and Node, K. (2009) Molecular basis of restenosis and novel issues of drug-eluting stents. *Circulation journal : official journal of the Japanese Circulation Society* **73**, 615-621
11. Nakahata, N. (2008) Thromboxane A2: physiology/pathophysiology, cellular signal transduction and pharmacology. *Pharmacology & therapeutics* **118**, 18-35
12. Montuschi, P., Barnes, P. J., and Roberts, L. J., 2nd. (2004) Isoprostanes: markers and mediators of oxidative stress. *FASEB journal : official publication of the Federation of American Societies for Experimental Biology* **18**, 1791-1800
13. Gluais, P., Lonchampt, M., Morrow, J. D., Vanhoutte, P. M., and Feletou, M. (2005) Acetylcholine-induced endothelium-dependent contractions in the SHR aorta: the Janus face of prostacyclin. *British journal of pharmacology* **146**, 834-845
14. Audoly, L. P., Rocca, B., Fabre, J. E., Koller, B. H., Thomas, D., Loeb, A. L., Coffman, T. M., and FitzGerald, G. A. (2000) Cardiovascular responses to the isoprostanes iPF(2alpha)-III and iPE(2)-III are mediated via the thromboxane A(2) receptor in vivo. *Circulation* **101**, 2833-2840
15. Ishimitsu, T., Uehara, Y., Ishii, M., Ikeda, T., Matsuoka, H., and Sugimoto, T. (1988)

Thromboxane and vascular smooth muscle cell growth in genetically hypertensive rats. *Hypertension* **12**, 46-51

16. Ishimitsu, T., Uehara, Y., Ishii, M., and Sugimoto, T. (1988) Enhanced generation of vascular thromboxane A2 in spontaneously hypertensive rats and its role in the rapid proliferation of vascular smooth muscle cells. *American journal of hypertension* **1**, 38S-40S
17. Hanasaki, K., Nakano, T., and Arita, H. (1990) Receptor-mediated mitogenic effect of thromboxane A2 in vascular smooth muscle cells. *Biochemical pharmacology* **40**, 2535-2542
18. Pakala, R., Willerson, J. T., and Benedict, C. R. (1997) Effect of serotonin, thromboxane A2, and specific receptor antagonists on vascular smooth muscle cell proliferation. *Circulation* **96**, 2280-2286
19. Pakala, R. (2004) Serotonin and thromboxane A2 stimulate platelet-derived microparticle-induced smooth muscle cell proliferation. *Cardiovascular radiation medicine* **5**, 20-26
20. Yokota, T., Shiraishi, R., Aida, T., Iwai, K., Liu, N. M., Yokoyama, U., and Minamisawa, S. (2014) Thromboxane A(2) receptor stimulation promotes closure of the rat ductus arteriosus through enhancing neointima formation. *PloS one* **9**, e94895
21. Owens, G. K., Kumar, M. S., and Wamhoff, B. R. (2004) Molecular regulation of vascular smooth muscle cell differentiation in development and disease. *Physiological reviews* **84**, 767-801
22. Cayatte, A. J., Du, Y., Oliver-Krasinski, J., Lavielle, G., Verbeuren, T. J., and Cohen, R. A. (2000) The thromboxane receptor antagonist S18886 but not aspirin inhibits atherogenesis in apo E-deficient mice: evidence that eicosanoids other than thromboxane contribute to atherosclerosis. *Arteriosclerosis, thrombosis, and vascular biology* **20**, 1724-1728
23. Kobayashi, T., Tahara, Y., Matsumoto, M., Iguchi, M., Sano, H., Murayama, T., Arai, H., Oida, H., Yurugi-Kobayashi, T., Yamashita, J. K., Katagiri, H., Majima, M., Yokode, M., Kita, T., and Narumiya, S. (2004) Roles of thromboxane A(2) and prostacyclin in the development of atherosclerosis in apoE-deficient mice. *J Clin Invest* **114**, 784-794
24. Egan, K. M., Wang, M., Fries, S., Lucitt, M. B., Zukas, A. M., Pure, E., Lawson, J. A., and FitzGerald, G. A. (2005) Cyclooxygenases, thromboxane, and atherosclerosis: plaque destabilization by cyclooxygenase-2 inhibition combined with thromboxane receptor antagonism. *Circulation* **111**, 334-342
25. Yu, F. X., Zhao, B., and Guan, K. L. (2015) Hippo Pathway in Organ Size Control, Tissue Homeostasis, and Cancer. *Cell* **163**, 811-828
26. Meng, Z., Moroishi, T., Mottier-Pavie, V., Plouffe, S. W., Hansen, C. G., Hong, A. W., Park, H. W., Mo, J.-S., Lu, W., Lu, S., Flores, F., Yu, F.-X., Halder, G., and Guan, K.-L. (2015) MAP4K family kinases act in parallel to MST1/2 to activate LATS1/2 in the Hippo pathway. *Nature Communications* **6**, 8357
27. Zheng, Y., Wang, W., Liu, B., Deng, H., Uster, E., and Pan, D. (2015) Identification of Happyhour/MAP4K as Alternative Hpo/Mst-like Kinases in the Hippo Kinase Cascade. *Developmental cell* **34**, 642-655
28. Dong, J., Feldmann, G., Huang, J., Wu, S., Zhang, N., Comerford, S. A., Gayyed, M. F., Anders, R. A., Maitra, A., and Pan, D. (2007) Elucidation of a universal size-control mechanism in Drosophila and mammals. *Cell* **130**, 1120-1133
29. Zhao, B., Wei, X., Li, W., Udan, R. S., Yang, Q., Kim, J., Xie, J., Ikenoue, T., Yu, J., Li, L.,

Zheng, P., Ye, K., Chinnaiyan, A., Halder, G., Lai, Z. C., and Guan, K. L. (2007) Inactivation of YAP oncoprotein by the Hippo pathway is involved in cell contact inhibition and tissue growth control. *Genes & development* **21**, 2747-2761

30. Lei, Q. Y., Zhang, H., Zhao, B., Zha, Z. Y., Bai, F., Pei, X. H., Zhao, S., Xiong, Y., and Guan, K. L. (2008) TAZ promotes cell proliferation and epithelial-mesenchymal transition and is inhibited by the hippo pathway. *Mol Cell Biol* **28**, 2426-2436
31. Zhao, B., Ye, X., Yu, J., Li, L., Li, W., Li, S., Yu, J., Lin, J. D., Wang, C. Y., Chinnaiyan, A. M., Lai, Z. C., and Guan, K. L. (2008) TEAD mediates YAP-dependent gene induction and growth control. *Genes & development* **22**, 1962-1971
32. Zhao, B., Li, L., Tumaneng, K., Wang, C. Y., and Guan, K. L. (2010) A coordinated phosphorylation by Lats and CK1 regulates YAP stability through SCF beta-TRCP. *Genes & development* **24**, 72-85
33. Harvey, K. F., Zhang, X., and Thomas, D. M. (2013) The Hippo pathway and human cancer. *Nature reviews. Cancer* **13**, 246-257
34. Miller, E., Yang, J., DeRan, M., Wu, C., Su, A. I., Bonamy, G. M., Liu, J., Peters, E. C., and Wu, X. (2012) Identification of serum-derived sphingosine-1-phosphate as a small molecule regulator of YAP. *Chemistry & biology* **19**, 955-962
35. Mo, J. S., Yu, F. X., Gong, R., Brown, J. H., and Guan, K. L. (2012) Regulation of the Hippo-YAP pathway by protease-activated receptors (PARs). *Genes & development* **26**, 2138-2143
36. Yu, F. X., Zhao, B., Panupinthu, N., Jewell, J. L., Lian, I., Wang, L. H., Zhao, J., Yuan, H., Tumaneng, K., Li, H., Fu, X. D., Mills, G. B., and Guan, K. L. (2012) Regulation of the Hippo-YAP pathway by G-protein-coupled receptor signaling. *Cell* **150**, 780-791
37. Wennmann, D. O., Vollenbroker, B., Eckart, A. K., Bonse, J., Erdmann, F., Wolters, D. A., Schenk, L. K., Schulze, U., Kremerskothen, J., Weide, T., and Pavenstadt, H. (2014) The Hippo pathway is controlled by Angiotensin II signaling and its reactivation induces apoptosis in podocytes. *Cell death & disease* **5**, e1519
38. Zhou, X., Wang, S. Y., Wang, Z., Feng, X., Liu, P., Lv, X. B., Li, F. L., Yu, F. X., Sun, Y. P., Yuan, H. X., Zhu, H. G., Xiong, Y., Lei, Q. Y., and Guan, K. L. (2015) Estrogen regulates Hippo signaling via GPER in breast cancer. *J Clin Invest* **125**, 2123-2135
39. Wang, X., Hu, G., Gao, X., Wang, Y., Zhang, W., Harmon, E. Y., Zhi, X., Xu, Z., Lennartz, M. R., Barroso, M., Trebak, M., Chen, C., and Zhou, J. (2012) The induction of yes-associated protein expression after arterial injury is crucial for smooth muscle phenotypic modulation and neointima formation. *Arteriosclerosis, thrombosis, and vascular biology* **32**, 2662-2669
40. Xie, C., Guo, Y., Zhu, T., Zhang, J., Ma, P. X., and Chen, Y. E. (2012) Yap1 protein regulates vascular smooth muscle cell phenotypic switch by interaction with myocardin. *The Journal of biological chemistry* **287**, 14598-14605
41. Dupont, S., Morsut, L., Aragona, M., Enzo, E., Giulitti, S., Cordenonsi, M., Zanconato, F., Le Digabel, J., Forcato, M., Bicciato, S., Elvassore, N., and Piccolo, S. (2011) Role of YAP/TAZ in mechanotransduction. *Nature* **474**, 179-183
42. Fernandez, B. G., Gaspar, P., Bras-Pereira, C., Jezowska, B., Rebelo, S. R., and Janody, F. (2011) Actin-Capping Protein and the Hippo pathway regulate F-actin and tissue growth in Drosophila. *Development* **138**, 2337-2346
43. Rauskolb, C., Pan, G., Reddy, B. V., Oh, H., and Irvine, K. D. (2011) Zyxin links fat signaling

to the hippo pathway. *PLoS biology* **9**, e1000624

44. Sansores-Garcia, L., Bossuyt, W., Wada, K., Yonemura, S., Tao, C., Sasaki, H., and Halder, G. (2011) Modulating F-actin organization induces organ growth by affecting the Hippo pathway. *Embo J* **30**, 2325-2335
45. Zhao, B., Li, L., Wang, L., Wang, C. Y., Yu, J., and Guan, K. L. (2012) Cell detachment activates the Hippo pathway via cytoskeleton reorganization to induce anoikis. *Genes & development* **26**, 54-68
46. Chan, E. H., Nousiainen, M., Chalamalasetty, R. B., Schafer, A., Nigg, E. A., and Sillje, H. H. (2005) The Ste20-like kinase Mst2 activates the human large tumor suppressor kinase Lats1. *Oncogene* **24**, 2076-2086
47. Marx, S. O., Totary-Jain, H., and Marks, A. R. (2011) Vascular smooth muscle cell proliferation in restenosis. *Circulation. Cardiovascular interventions* **4**, 104-111
48. Ricciotti, E., and FitzGerald, G. A. (2011) Prostaglandins and inflammation. *Arteriosclerosis, thrombosis, and vascular biology* **31**, 986-1000
49. Smyth, E. M., Grosser, T., Wang, M., Yu, Y., and FitzGerald, G. A. (2009) Prostanoids in health and disease. *Journal of lipid research* **50 Suppl**, S423-428
50. Fetalvero, K. M., Shyu, M., Nomikos, A. P., Chiu, Y. F., Wagner, R. J., Powell, R. J., Hwa, J., and Martin, K. A. (2006) The prostacyclin receptor induces human vascular smooth muscle cell differentiation via the protein kinase A pathway. *American journal of physiology. Heart and circulatory physiology* **290**, H1337-1346
51. Yu, F. X., Zhang, Y. F., Park, H. W., Jewell, J. L., Chen, Q., Deng, Y. T., Pan, D. J., Taylor, S. S., Lai, Z. C., and Guan, K. L. (2013) Protein kinase A activates the Hippo pathway to modulate cell proliferation and differentiation. *Genes & development* **27**, 1223-1232
52. Bauer, J., Ripperger, A., Frantz, S., Ergun, S., Schwedhelm, E., and Benndorf, R. A. (2014) Pathophysiology of isoprostanes in the cardiovascular system: implications of isoprostane-mediated thromboxane A2 receptor activation. *British journal of pharmacology* **171**, 3115-3131
53. Peterson, M. B., Machaj, V., Block, P. C., Palacios, I., Philbin, D., and Watkins, W. D. (1986) Thromboxane release during percutaneous transluminal coronary angioplasty. *American heart journal* **111**, 1-6
54. Cicha, I., Yilmaz, A., Klein, M., Raithel, D., Brigstock, D. R., Daniel, W. G., Goppelt-Struebe, M., and Garlichs, C. D. (2005) Connective tissue growth factor is overexpressed in complicated atherosclerotic plaques and induces mononuclear cell chemotaxis in vitro. *Arteriosclerosis, thrombosis, and vascular biology* **25**, 1008-1013
55. Matsumae, H., Yoshida, Y., Ono, K., Togi, K., Inoue, K., Furukawa, Y., Nakashima, Y., Kojima, Y., Nobuyoshi, M., Kita, T., and Tanaka, M. (2008) CCN1 knockdown suppresses neointimal hyperplasia in a rat artery balloon injury model. *Arteriosclerosis, thrombosis, and vascular biology* **28**, 1077-1083
56. Lee, H. Y., Chung, J. W., Youn, S. W., Kim, J. Y., Park, K. W., Koo, B. K., Oh, B. H., Park, Y. B., Chaqour, B., Walsh, K., and Kim, H. S. (2007) Forkhead transcription factor FOXO3a is a negative regulator of angiogenic immediate early gene CYR61, leading to inhibition of vascular smooth muscle cell proliferation and neointimal hyperplasia. *Circ Res* **100**, 372-380
57. Michels, S., and Schmidt-Erfurth, U. (2001) Photodynamic therapy with verteporfin: a new treatment in ophthalmology. *Seminars in ophthalmology* **16**, 201-206

58. Liu-Chittenden, Y., Huang, B., Shim, J. S., Chen, Q., Lee, S. J., Anders, R. A., Liu, J. O., and Pan, D. J. (2012) Genetic and pharmacological disruption of the TEAD-YAP complex suppresses the oncogenic activity of YAP. *Genes & development* **26**, 1300-1305
59. Lv, X. B., Liu, C. Y., Wang, Z., Sun, Y. P., Xiong, Y., Lei, Q. Y., and Guan, K. L. (2015) PARD3 induces TAZ activation and cell growth by promoting LATS1 and PP1 interaction. *EMBO reports* **16**, 975-985
60. Ray, J. L., Leach, R., Herbert, J. M., and Benson, M. (2001) Isolation of vascular smooth muscle cells from a single murine aorta. *Methods in cell science : an official journal of the Society for In Vitro Biology* **23**, 185-188

FOOTNOTES

This work was supported by the National Natural Science Foundation of China (No. 31570784 to H.X.Y.). Y.X. is supported by grants from National Institute of Health (RO1GM067113, RO1CA068377 and RO1CA163834), K.L.G. is supported by grants from National Institute of Health (R35CA196878, RO1GM51586, and RO1EY022611).

FIGURE LEGENDS

Figure 1. Agonists of TP receptor activate YAP and TAZ.
(A-B) I-BOP induces YAP and TAZ dephosphorylation in a dose- and time-dependent manner in Hela cells. Cells were serum-starved for 16 h and then stimulated with I-BOP for the concentration (A) or time (B) as indicated. Immunoblotting were performed with the indicated antibodies. Phos-tag gels were used for assessment of TAZ phosphorylation status. (C) I-BOP and U-46619 induce YAP nuclear accumulation in HeLa cells. HeLa cells were seeded with a density of 6×10^4 cells/cm^2 for 12 h then starved in serum-free medium for 16 h and stimulated with 1 nmol/L I-BOP or 10 nmol/L U-46619 for 1 h. YAP subcellular localization was determined by immunofluorescence staining for endogenous YAP (green); DAPI (blue) was used for staining cell nuclei. Representative images are shown. Scale bar, 20 μm. Quantifications are shown in the right panel. (D) I-BOP and U-46619 induce YAP/TAZ nuclear accumulation in HeLa cells. HeLa cells were seeded with a density of 6×10^4 cells/cm^2 for 12 h then starved in serum-free medium for 16 h and stimulated with 1 nmol/L I-BOP or 10 nmol/L U-46619 for 1 h. Subcellular fractionation was performed with NE-PER™ Nuclear and Cytoplasmic Extraction Reagents (ThermoFisher) according to the manufacturer's instructions. Both fractions were analyzed by Western blot with indicated antibodies. (E) I-BOP and U-46619 enhance YAP interaction with TEAD1. Cell lysates were subjected to immunoprecipitation with YAP antibody. The coimmunoprecipitated TEAD1 was detected by immunoblotting. (F-G) I-BOP induces YAP/TAZ dephosphorylation in a dose- and time-dependent manner in T/G HA-VSMCs. Cells were serum-starved for 16 h and then stimulated with I-BOP for the concentration (F) or time (G) as indicated. Immunoblotting were performed with the indicated antibodies. Phos-tag gels were used for assessment of YAP/TAZ phosphorylation status. (H) I-BOP induces Yap/Taz dephosphorylation in a dose-dependent manner in primary MAVSMCs. Cells were serum-starved for 16 h and then stimulated with I-BOP for the concentration as indicated. FBS was included as a positive control. Immunoblotting were performed with the indicated antibodies. Phos-tag gels were used for assessment of Yap and Taz phosphorylation status. (I) I-BOP induces expression of YAP target genes. T/G HA-VSMCs were treated with 1 nmol/L I-BOP for 2 h after serum-starved for 16 h. mRNA levels of CTGF, CYR61, TAGLN, and EDN1 were measured by quantitative PCR.

Figure 2. TP agonist activates YAP/TAZ via TP receptor and $G\alpha_{12/13}$.
(A) TP antagonist SQ-29548 blocks YAP/TAZ dephosphorylation induced by I-BOP. Serum-starved T/G HA-VSMCs were pretreated with TP specific antagonist SQ-29548 (1 μmol/L) for 3h and then stimulated with I-BOP (1 nmol/L) for 1 h. Cell lysates were subjected to immunoblotting with the indicated antibodies. (B) Ectopic expression of TPα receptor renders HEK293A cells sensitive to I-BOP treatment. HEK293A cells were transiently transfected with the indicated plasmids and were stimulated with different concentrations of I-BOP for 1 h. Immunoblotting was performed with the indicated antibodies. (C) Knockout of *TP* (*TP*-KO) blocks I-BOP-induced YAP/TAZ dephosphorylation. Wild-type or *TP*-KO HEK293A cells, which were verified by genomic DNA sequencing (Supplemental Figure 3), were seeded with a density of 8×10^4 cells/cm^2 for 24 h then treated with 10 nmol/L I-BOP for 1 h. Immunoblotting was performed with the indicated antibodies. (D) *TP*-KO abolishes I-BOP-induced YAP nuclear translocation. Stimulation conditions were same to those in panel C, YAP localization was determined by immunofluorescence. Scale bar, 30 μm (E) *TP*-KO blocks I-BOP-induced target genes expression. Wild-type or *TP*-KO HEK293A cells were

treated with 10 nmol/L I-BOP for 2 h. mRNA levels of CTGF and CYR61 were measured by quantitative PCR. (F) I-BOP activates YAP/TAZ via $G\alpha_{12/13}$. HEK293A cells were transfected with the indicated siRNAs. A mixture of two independent oligonucleotides was used for one gene. Two days after transfection, cells were treated with 10 nmol/L I-BOP for 1 h. cells were lysed and subjected to immunoblotting with the indicated antibodies. (G) Knockdown of $G\alpha_{12/13}$ blocks I-BOP-induced YAP nuclear localization. Stimulation conditions were similar to those in panel F. Immunofluorescence staining for endogenous YAP (green) and F-actin (red); DNA (blue) are presented. Scale bar, 20 μm.

Figure 3. I-BOP activates YAP/TAZ through Rho and cytoskeletons.
(A) I-BOP-induced YAP/TAZ dephosphorylation is blocked by Rho-GDI expression. HEK293A cells were transiently transfected with the indicated plasmids and were incubated with 10 nmol/L I-BOP for 1 h. Immunoblotting was performed with the indicated antibodies. (B) Inactivation of Rho by C3 prevents YAP/TAZ dephosphorylation. Serum-starved T/G HA-VSMCs were pretreated with C3 (4 μg/ml) for 3 h and then stimulated with I-BOP (1 nmol/L) for 1 h. The cell lysates were subjected to immunoblotting analysis with the indicated antibodies. (C) Inactivation of Rho by C3 prevents YAP nuclear accumulation. Serum-starved HEK293A cells were pretreated with C3 (2 μg/ml) for 3 h and then stimulated with I-BOP (10 nmol/L) for 1 h. After fixation, immunofluorescence staining was performed for endogenous YAP (green), F-actin (red); DAPI (blue) was used for staining cell nuclei. Scale bar, 20 μm. (D) Disruption of actin-cytoskeleton blocks I-BOP-induced YAP/TAZ dephosphorylation. Serum-starved T/G HA-VSMCs were pretreated with LatB (1 μg/ml) for 10 min and then stimulated with I-BOP (1 nmol/L) for the indicated time. The cell lysates were subjected to immunoblotting analysis with the indicated antibodies. (E) Disruption of actin-cytoskeleton blocks I-BOP-induced YAP nuclear localization. HEK293A cells were pretreated with Latrunculin B (1 μg/ml) for 10 min and then stimulated with I-BOP (10 nmol/L) for the indicated time. Immunofluorescence staining is similar to that shown in panel C. Scale bar, 20 μm.

Figure 4. I-BOP inhibits LATS.
(A) I-BOP inhibits the activation loop phosphorylation of LATS1 in a Rho-dependent manner. HEK293A cells were pretreated with C3 (2 μg/mL) for 3 h and then stimulated with I-BOP (10 nmol/L) for 1 h. The presence of FBS is indicated. Cell lysates were subjected to immunoprecipitation with control IgG or LATS1 antibody. The immunoprecipitated LATS1 was measured for *in vitro* kinase assays using GST-YAP as a substrate. The phosphorylation of LATS1 and GST-YAP were detected by immunoblotting with the indicated antibodies. (B) MST1/2 are not essential for I-BOP-induced YAP/TAZ dephosphorylation. Wild-type or MST1/2-dKO HEK293A cells were treated with I-BOP (10 nmol/L) for the indicated time points. The cell lysates were subjected to immunoblotting with the indicated antibodies. (C) Both MST1/2 and MAP4Ks are involved in I-BOP-induced YAP/TAZ dephosphorylation. Wild-type or MM-9KO HEK293A cells, which were verified by genomic DNA sequencing (Supplemental Figure 7), were treated with I-BOP (10 nmol/L) for the indicated time. The cell lysates were subjected to immunoblotting as indicated. (D) Re-expression of MST1/2 or MAP4K2 in MM-9KO cells restores I-BOP-induced YAP/TAZ dephosphorylation. Wild-type or MM-9KO HEK293A cells were transfected with the indicated plasmids and treated with I-BOP (10 nmol/L) for 1 h. The cell lysates were subjected to immunoblotting as indicated. (E) MST1/2 and MAP4Ks are required for I-BOP to induce LATS

inhibition. Wild-type or MM-9KO HEK293A cells were transfected with the indicated plasmids and treated with I-BOP (10 nmol/L) for 1 h. The Cell lysates were subjected to immunoprecipitation with Flag-beads. The immunoprecipitated Flag-LATS1 was measured for *in vitro* kinase assays using GST-YAP as a substrate. The phosphorylation of LATS1 and GST-YAP were detected by immunoblotting with the indicated antibodies.

Figure 5. YAP/TAZ mediate the effect of TP in gene induction, DNA synthesis and cell migration in VSMCs. (A) Knockdown of YAP/TAZ by shRNAs and siRNAs in T/G HA-VSMCs. Cells were transfected with the indicated siRNAs. 48 h after transfection and doxycycline induction, cells were lysed and subjected to immunoblotting with the indicated antibodies. (B) YAP/TAZ are required for I-BOP-induced gene expression. T/G HA-VSMCs were transfected with the indicated siRNAs and serum-starved for 24h in the presence of doxycycline. After treating with I-BOP (1 nmol/L) for 1 h, mRNA level of CTGF and CYR61 were measured by real-time PCR. The Arabic numbers next to each treatment conditions will be used to label panels C-E. (C) YAP/TAZ are required for I-BOP-induced cell migration. The treatment conditions for each panel are same as in panel B. After stimulated with I-BOP (1 nmol/L) for 4 h, cell migration was performed by transwell cell migration assay. Representative images are shown. (D) The quantification result of the data in panel C. An asterisk indicates a statistically significant difference ($P < 0.05$). Statistical analysis is described in the Materials and Methods. (E) YAP/TAZ are required for I-BOP-induced DNA synthesis. T/G HA-VSMCs were treated as indicated in panel B and then performed EdU incorporation assay as described in Methods. About 600-1000 randomly selected cells are quantified and shown. An asterisk indicates a statistically significant difference ($P < 0.05$). (F) Yap/Taz knockdown by siRNAs in primary MAVSMCs. Cells were transfected with the indicated siRNAs. After 48 h transfection, cells were lysed and subjected to immunoblotting with the indicated antibodies. (G) Yap/Taz are required for primary MAVSMCs migration induced by I-BOP. The primary MAVSMCs were transfected with the indicated siRNAs and serum-starved for 20h. After stimulation with I-BOP (1 nmol/L) for 4 h, cell migration was determined by transwell cell migration assay. Representative images are shown. (H) Quantification result of the data in panel G. An asterisk indicates a statistically significant difference ($P < 0.05$).

Figure 6. A proposed model for thromboxane A2 receptor in the regulation of YAP/TAZ activities.

Figure 1

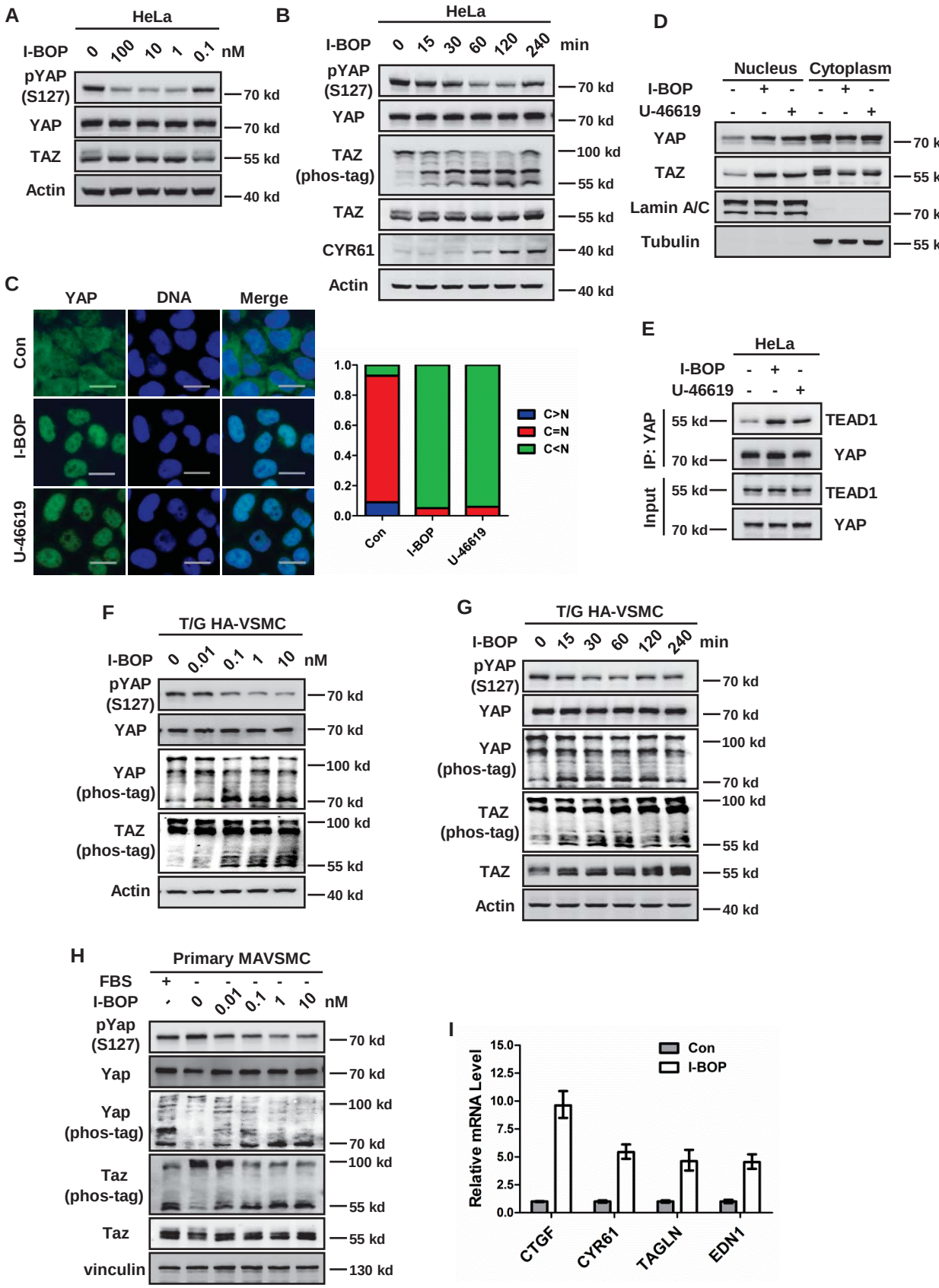
A
HeLa
I-BOP 0 100 10 1 0.1 nM
pYAP (S127)
YAP
TAZ
Actin
70 kd
70 kd
55 kd
40 kd
B
HeLa
I-BOP 0 15 30 60 120 240 min
pYAP (S127)
YAP
TAZ (phos-tag)
TAZ
CYR61
Actin
70 kd
70 kd
100 kd
55 kd
55 kd
40 kd
40 kd
D
Nucleus Cytoplasm
I-BOP - + - - + -
U-46619 - - + - - +
YAP
TAZ
Lamin A/C
Tubulin
70 kd
55 kd
70 kd
55 kd
C
YAP DNA Merge
Con
I-BOP
U-46619
1.0
0.8
0.6
0.4
0.2
0.0
C>N
C=N
C<N
Con
I-BOP
U-46619
E
HeLa
I-BOP - + -
U-46619 - - +
IP: YAP
55 kd
70 kd
TEAD1
YAP
Input
55 kd
70 kd
TEAD1
YAP
F
T/G HA-VSMC
I-BOP 0 0.01 0.1 1 10 nM
pYAP (S127)
YAP
YAP (phos-tag)
TAZ (phos-tag)
Actin
70 kd
70 kd
100 kd
70 kd
100 kd
55 kd
40 kd
G
T/G HA-VSMC
I-BOP 0 15 30 60 120 240 min
pYAP (S127)
YAP
YAP (phos-tag)
TAZ (phos-tag)
TAZ
Actin
70 kd
70 kd
100 kd
70 kd
100 kd
55 kd
55 kd
40 kd
H
Primary MAVSMC
FBS + - - - - -
I-BOP - 0 0.01 0.1 1 10 nM
pYap (S127)
Yap
Yap (phos-tag)
Taz (phos-tag)
Taz
vinculin
70 kd
70 kd
100 kd
70 kd
100 kd
55 kd
55 kd
130 kd
I
Relative mRNA Level
15.0
12.5
10.0
7.5
5.0
2.5
0.0
Con
I-BOP
CTGF
CYR61
TAGLN
EDN1

Figure 2

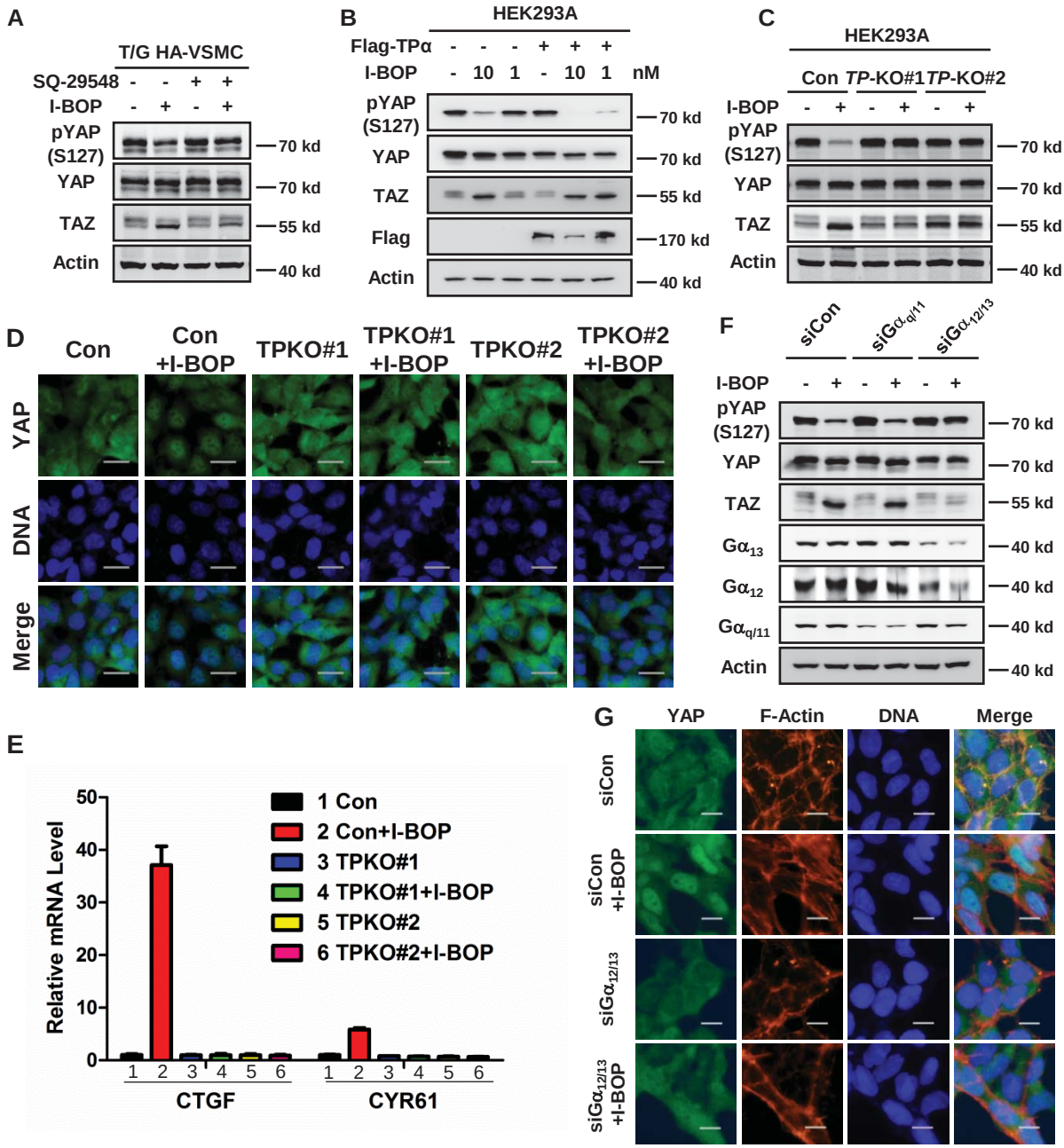
A
T/G HA-VSMC
SQ-29548 - - + +
I-BOP - + - +
pYAP (S127)
YAP
TAZ
Actin
70 kd
70 kd
55 kd
40 kd
B
HEK293A
Flag-TPα - - - + + +
I-BOP - 10 1 - 10 1 nM
pYAP (S127)
YAP
TAZ
Flag
Actin
70 kd
70 kd
55 kd
170 kd
40 kd
C
HEK293A
Con TP-KO#1 TP-KO#2
I-BOP - + - + - +
pYAP (S127)
YAP
TAZ
Actin
70 kd
70 kd
55 kd
40 kd
D
Con
Con +I-BOP
TPKO#1
TPKO#1 +I-BOP
TPKO#2
TPKO#2 +I-BOP
YAP
DNA
Merge
F
siCon
siGαq/11
siGα12/13
I-BOP - + - + - +
pYAP (S127)
YAP
TAZ
Gα13
Gα12
Gαq/11
Actin
70 kd
70 kd
55 kd
40 kd
40 kd
40 kd
40 kd
E
Relative mRNA Level
50
40
30
20
10
0
1 Con
2 Con+I-BOP
3 TPKO#1
4 TPKO#1+I-BOP
5 TPKO#2
6 TPKO#2+I-BOP
1 2 3 4 5 6
CTGF
1 2 3 4 5 6
CYR61
G
YAP
F-Actin
DNA
Merge
siCon
siCon +I-BOP
siGα12/13
siGα12/13 +I-BOP

Figure 3

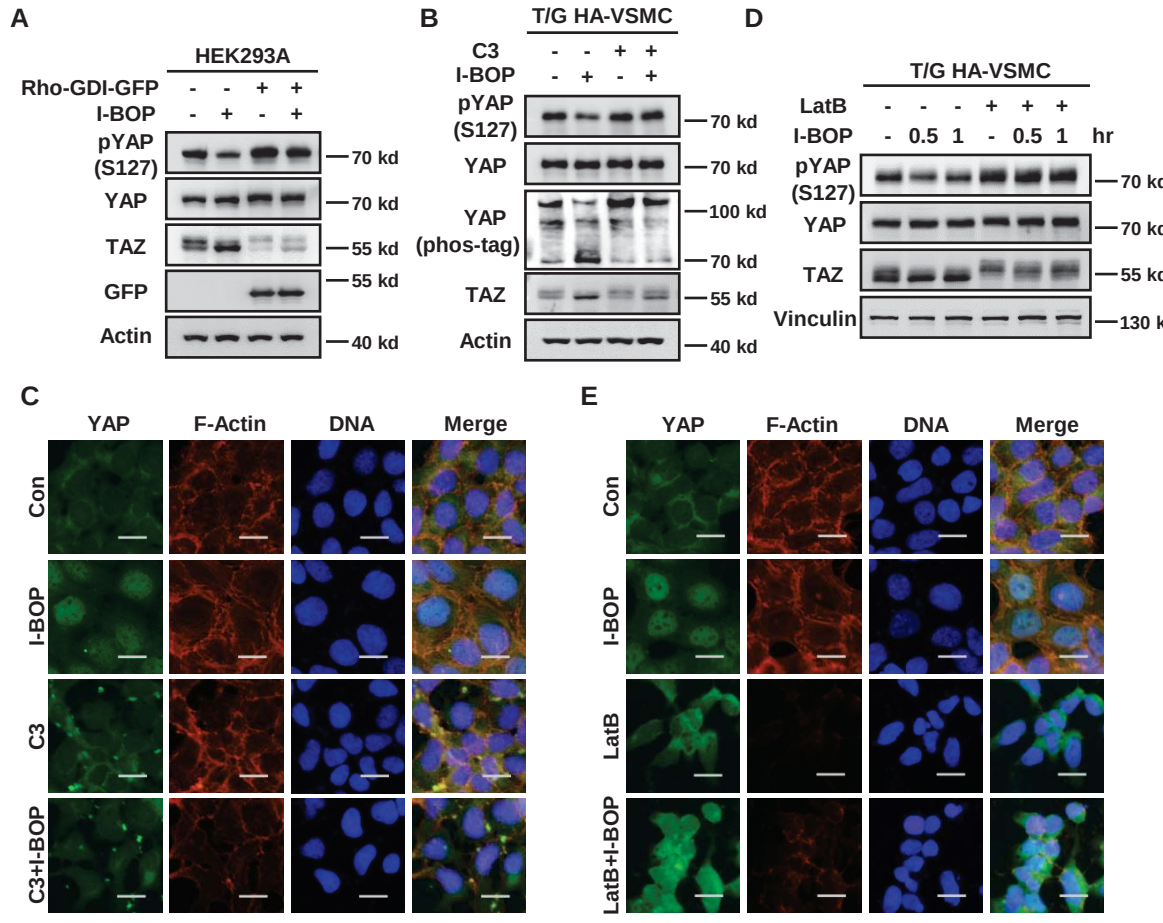
A
HEK293A
Rho-GDI-GFP - - + +
I-BOP - + - +
pYAP (S127)
YAP
TAZ
GFP
Actin
70 kd
70 kd
55 kd
55 kd
40 kd
B
T/G HA-VSMC
C3 - - + +
I-BOP - + - +
pYAP (S127)
YAP
YAP (phos-tag)
TAZ
Actin
70 kd
70 kd
100 kd
70 kd
55 kd
40 kd
D
T/G HA-VSMC
LatB - - - + + +
I-BOP - 0.5 1 - 0.5 1 hr
pYAP (S127)
YAP
TAZ
Vinculin
70 kd
70 kd
55 kd
130 kd
C
YAP
F-Actin
DNA
Merge
Con
I-BOP
C3
C3+I-BOP
E
YAP
F-Actin
DNA
Merge
Con
I-BOP
LatB
LatB+I-BOP

Figure 4

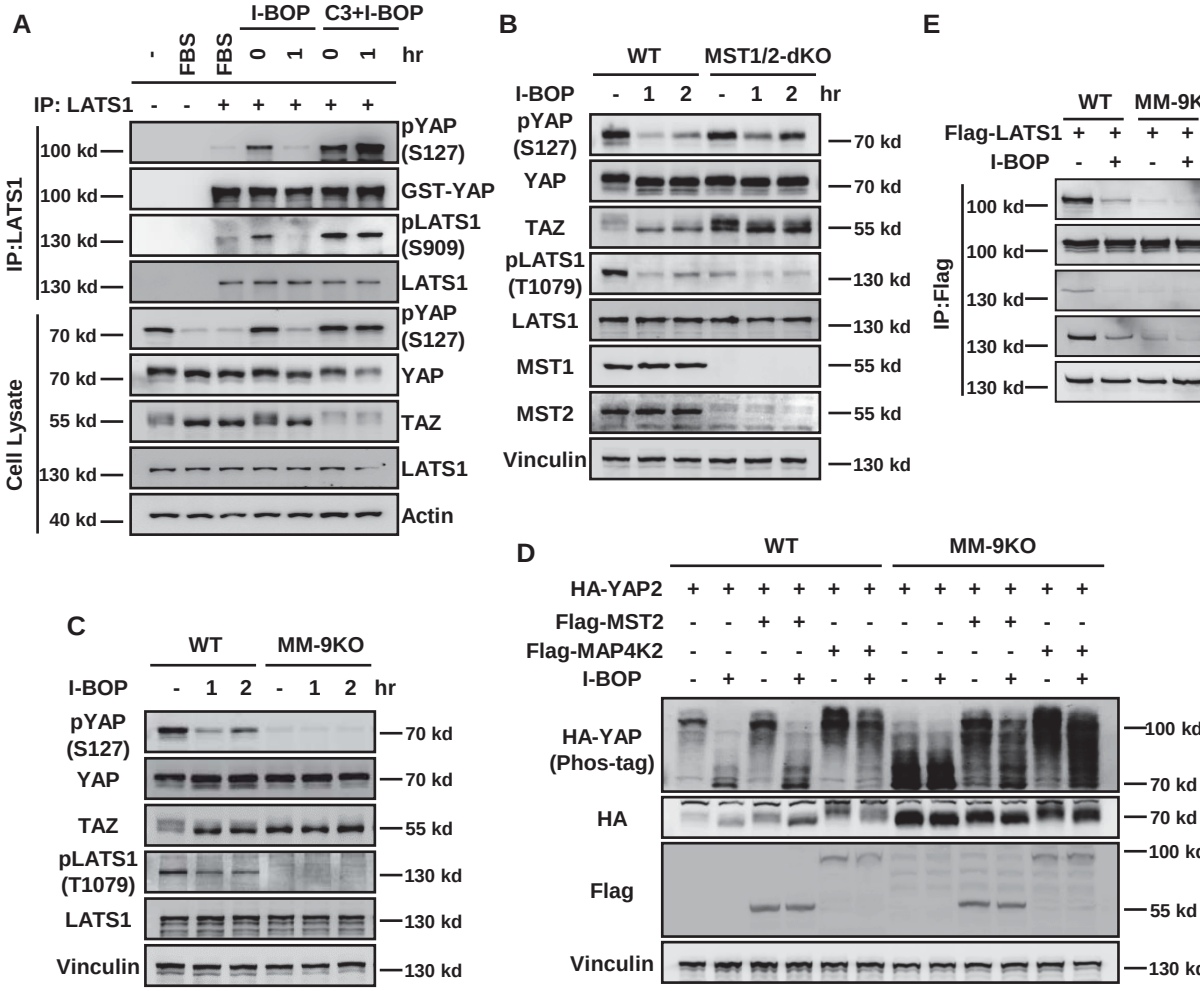
A
I-BOP
C3+I-BOP
-
FBS
FBS
0
1
0
1
hr
IP: LATS1 - - + + + + +
IP:LATS1
100 kd
pYAP (S127)
100 kd
GST-YAP
130 kd
pLATS1 (S909)
130 kd
LATS1
Cell Lysate
70 kd
pYAP (S127)
70 kd
YAP
55 kd
TAZ
130 kd
LATS1
40 kd
Actin
B
WT
MST1/2-dKO
I-BOP - 1 2 - 1 2 hr
pYAP (S127)
70 kd
YAP
70 kd
TAZ
55 kd
pLATS1 (T1079)
130 kd
LATS1
130 kd
MST1
55 kd
MST2
55 kd
Vinculin
130 kd
E
WT
MM-9KO
Flag-LATS1 + + + +
I-BOP - + - +
IP:Flag
100 kd
pYAP (S127)
100 kd
GST-YAP
130 kd
pLATS1 (S909)
130 kd
pLATS1 (T1079)
130 kd
LATS1
C
WT
MM-9KO
I-BOP - 1 2 - 1 2 hr
pYAP (S127)
70 kd
YAP
70 kd
TAZ
55 kd
pLATS1 (T1079)
130 kd
LATS1
130 kd
Vinculin
130 kd
D
WT
MM-9KO
HA-YAP2 + + + + + + + + + + + +
Flag-MST2 - - + + - - - - + + - -
Flag-MAP4K2 - - - - + + - - - - + +
I-BOP - + - + - + - + - + - +
HA-YAP (Phos-tag)
100 kd
70 kd
HA
70 kd
Flag
100 kd
55 kd
Vinculin
130 kd

Figure 5

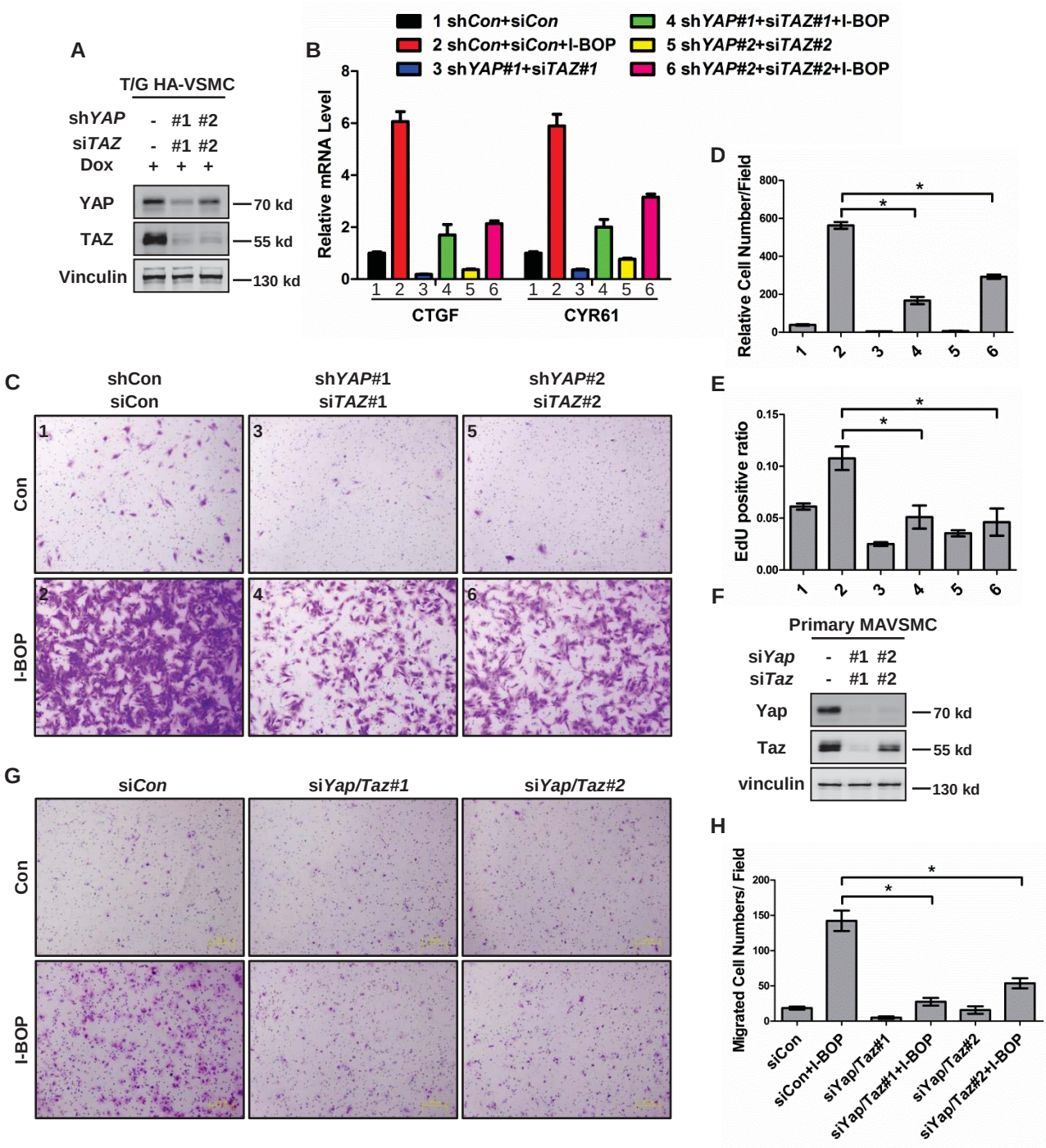
A
T/G HA-VSMC
shYAP - #1 #2
siTAZ - #1 #2
Dox + + +
YAP
TAZ
Vinculin
70 kd
55 kd
130 kd
B
1 shCon+siCon
2 shCon+siCon+I-BOP
3 shYAP#1+siTAZ#1
4 shYAP#1+siTAZ#1+I-BOP
5 shYAP#2+siTAZ#2
6 shYAP#2+siTAZ#2+I-BOP
Relative mRNA Level
CTGF
CYR61
C
shCon
siCon
shYAP#1
siTAZ#1
shYAP#2
siTAZ#2
Con
I-BOP
D
Relative Cell Number/Field
E
EdU positive ratio
F
Primary MAVSMC
siYap - #1 #2
siTaz - #1 #2
Yap
Taz
vinculin
70 kd
55 kd
130 kd
G
siCon
siYap/Taz#1
siYap/Taz#2
Con
I-BOP
H
Migrated Cell Numbers/ Field
siCon
siCon+I-BOP
siYap/Taz#1
siYap/Taz#1+I-BOP
siYap/Taz#2
siYap/Taz#2+I-BOP

Figure 6

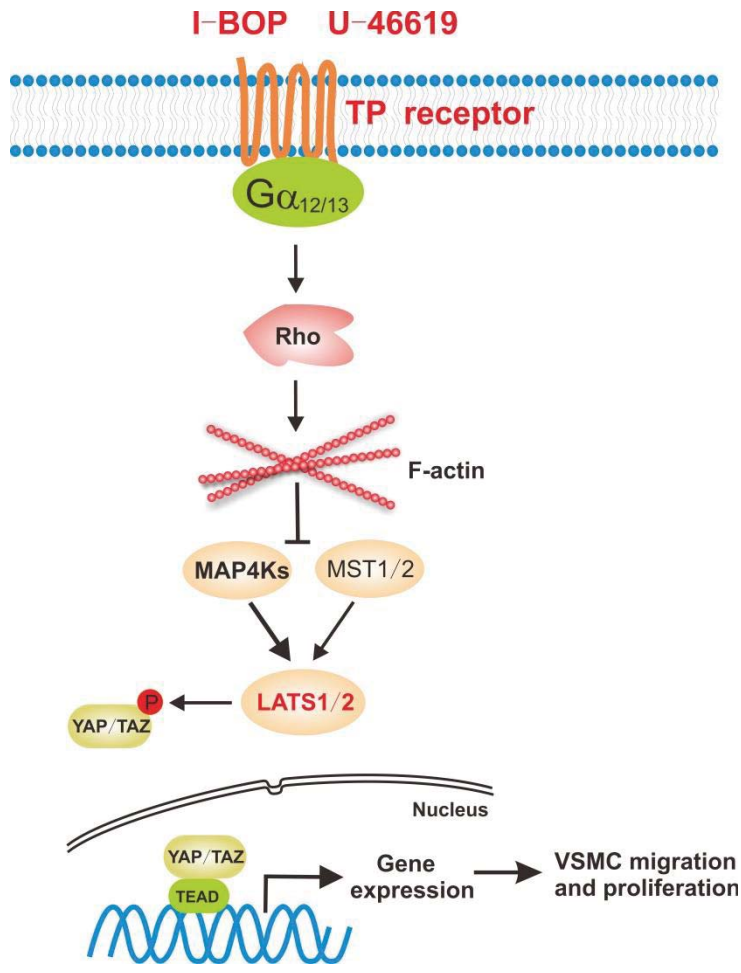
I-BOP
U-46619
TP receptor
Gα12/13
Rho
F-actin
MAP4Ks
MST1/2
LATS1/2
P
YAP/TAZ
Nucleus
YAP/TAZ
TEAD
Gene expression
VSMC migration and proliferation

SUPPLEMENTAL FIGURE LEGENDS

Supplemental Figure 1. TP induces dephosphorylation of YAP and TAZ.
(A-B) U-46619 induces YAP/TAZ dephosphorylation in HeLa cells. Cells were serum-starved for 16 h and then stimulated with U-46619 for the concentration (A) or time (B) as indicated. Immunoblotting were performed with the indicated antibodies. (C) Both I-BOP and U-46619 cause TAZ nuclear accumulation. HeLa cells were serum-starved for 16 h and then stimulated with 1 nmol/L I-BOP or 10 nmol/L U-46619 for 1 h. After fixation, TAZ subcellular localization was determined by immunofluorescence staining for endogenous TAZ (green); DAPI (blue) was used for cell nuclei. Representative images are shown. Scale bar, 20 μm. (D and E) Both U-46619 and I-BOP promote YAP target genes transcription. HeLa cells were treated with 10 nmol/L U-46619 for 1 h (H) or 1 nmol/L I-BOP for 2 h (I) after serum-starved for 16 h. mRNA levels of CTGF, CYR61, TAGLN, EDN1 and ANKRD1 were measured by quantitative PCR. (F-I) Effect of I-BOP on YAP/TAZ phosphorylation in different cell lines. Cells were serum-starved for 16 h and then stimulated with different concentrations of I-BOP for 1 h (2 h for MDA-MB-231) (F-H) or stimulated with different time with 10 nmol/L I-BOP (I). cell lysates prepared from different cells lines were used for immunoblotting. F, MDA-MB-231 cells. G, SW480 cells. H and I, HEK293A cells.

Supplemental Figure 2. TP agonist U-46619 activates YAP/TAZ via both isoforms of TP receptor.
Overexpression of TPα/β receptor renders YAP/TAZ sensitive to U-46619 treatment. U2OS cells stably expressing TPα/β and control cells were incubated with 10 nmol/L U-46619 for 1 h. Cell lysates were subjected to immunoblotting with the indicated antibodies. TAZ phosphorylation was determined by phos-tag. TPα/β receptor expression was determined by RT-PCR with their specific primers respectively.

Supplemental Figure 3. Verification of HEK293A cell lines with TP deletion.
Alignment of *TP*-KO cell line with WT cells. Both clones are heterozygous. Clone *TP*-KO#1: the two alleles contain one or two nucleotides insertion respectively. Clone *TP*-KO#2: one allele contains two nucleotides deletion, while the other allele contains 56 nucleotides insertion.

Supplemental Figure 4. Knockdown of Gαq/11 has little effect on I-BOP-induced YAP nuclear localization. HEK293A cells were transfected with the indicated siRNAs. A mixture of two independent oligonucleotides was used for one gene. After 48 h transfection, cells were treated with 10 nmol/L I-BOP for 1 h. Immunofluorescence staining for endogenous YAP (green) and F-actin (red); DAPI (blue) was used for cell nuclei. Scale bar, 20 μm.

Supplemental Figure 5. TP agonists activate YAP/TAZ through Rho and cytoskeletons.
(A and B) Inactivation of Rho by C3 prevents YAP/TAZ dephosphorylation. Serum-starved HEK293A and HeLa cells were pretreated with C3 (2μg/ml for HEK293A, 4μg/ml for HeLa) for 3 h and then stimulated with 10 nmol/L I-BOP or U-46619 as indicated for 1 h. The cell lysates were subjected to immunoblotting analysis with the indicated antibodies. (C) Inactivation of Rho by C3 prevents YAP nuclear accumulation. Serum-starved HeLa cells were pretreated with C3 (4μg/ml) for 3 h and then stimulated with 10 nmol/L U-46619 for 1 h. After fixation, immunofluorescence staining was performed

for endogenous YAP (green), F-actin (red); DAPI (blue) was used for cell nuclei. Scale bars, 20 μm. (D, E) Disruption of actin-cytoskeleton blocks I-BOP-induced YAP/TAZ dephosphorylation and nuclear localization. Serum-starved HeLa cells were pretreated with Latrunculin B (1μg/ml) for 10 min and then stimulated with 10 nmol/L U-46619 for 1 h. (D) The cell lysates were subjected to immunoblotting analysis with the indicated antibodies. (E) Immunofluorescence staining is similar to that shown in C. Scale bar, 20 μm.

Supplemental Figure 6. LATS1/2 are required for the effect of I-BOP on YAP/TAZ phosphorylation.
Wild-type or LATS1/2-dKO HEK293A cells were treated with I-BOP (10 nmol/L) for the indicated time points. The cell lysates were subjected to immunoblotting as indicated.

Supplemental Figure 7. Verification of HEK293A cell lines with MAP4K5 deletion in MM-8KO cells. Alignment of MM-9KO cell line with WT cells. The clone is heterozygous. one allele contains 1 nucleotide deletion, while the other allele contains 1 nucleotide insertion.

Supplemental Figure 8. YAP/TAZ mediate physiological function of TP in gene induction, DNA synthesis and cell migration.
(A) YAP/TAZ are required for I-BOP-induced DNA synthesis. T/G HA-VSMCs were treated as indicated and then performed EdU incorporation assay as described in Materials and Methods. Representative images are shown. (B) *YAP/TAZ* knockdown by siRNAs in HeLa cells. HeLa cells were transfected with the indicated siRNAs. A mixture of two independent oligonucleotides was used for one gene. After 48 h transfection, cells were lysed and subjected to immunoblotting with the indicated antibodies. (C) YAP/TAZ are required for I-BOP-induced gene expression. HeLa cells were transfected with the indicated siRNAs and serum-starved for 16 h, then treated with 1 nmol/L I-BOP for 2 h. mRNA level of CTGF, CYR61, TAGLN, ANKRD1, and EDN1 were measured by real-time PCR. (D) YAP/TAZ are required for I-BOP-induced cell migration. HeLa cells were transfected with the indicated siRNAs. After serum starvation for 20 h, cells were treated with 1 nmol/L I-BOP for 4 h. Cell migration was performed by transwell cell migration assay. Representative images are shown and the quantification is shown in the right panel. An asterisk indicates a statistically significant difference ($P < 0.05$).

Supplemental Figure 1

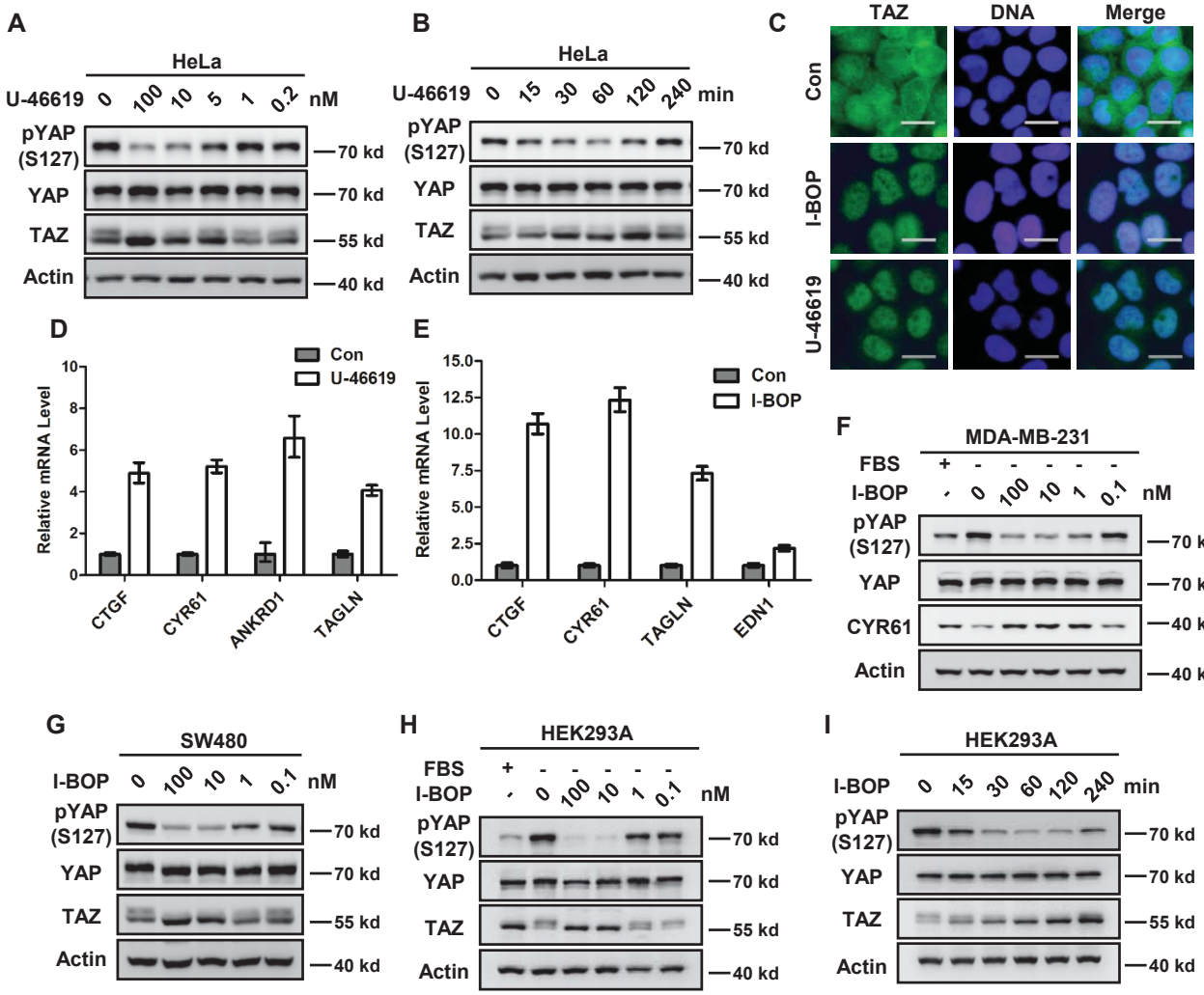

Supplemental Figure 2

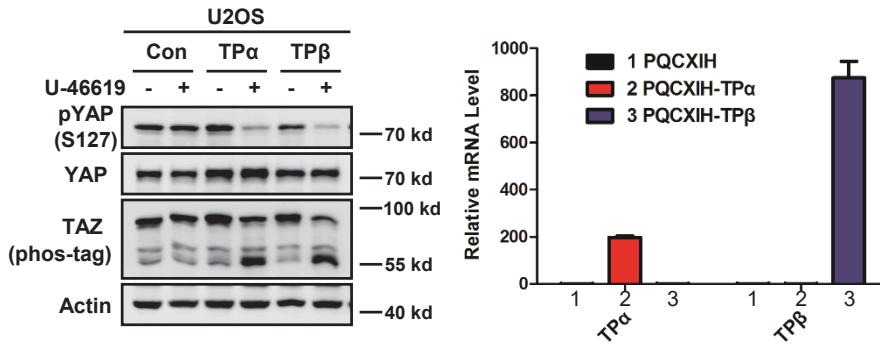

Supplemental Figure 3

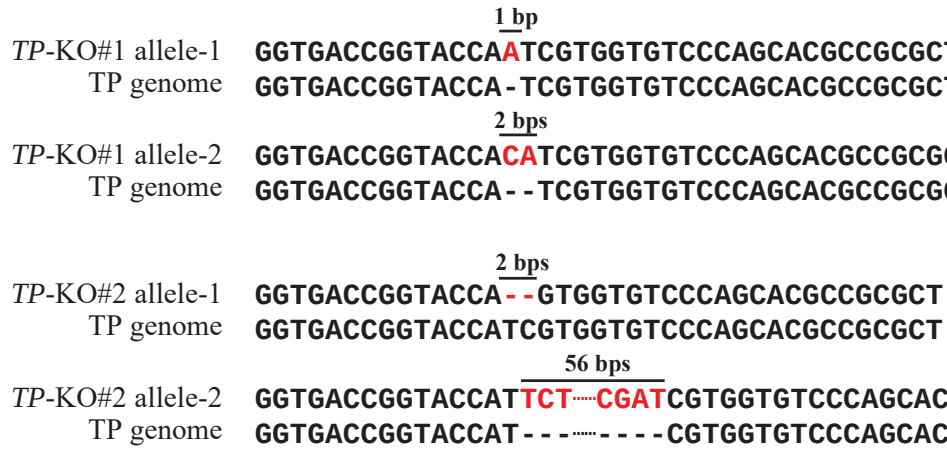

Supplemental Figure 4

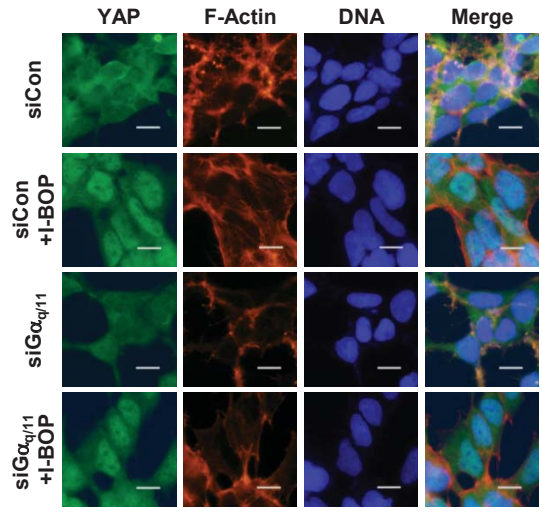

Supplemental Figure 5

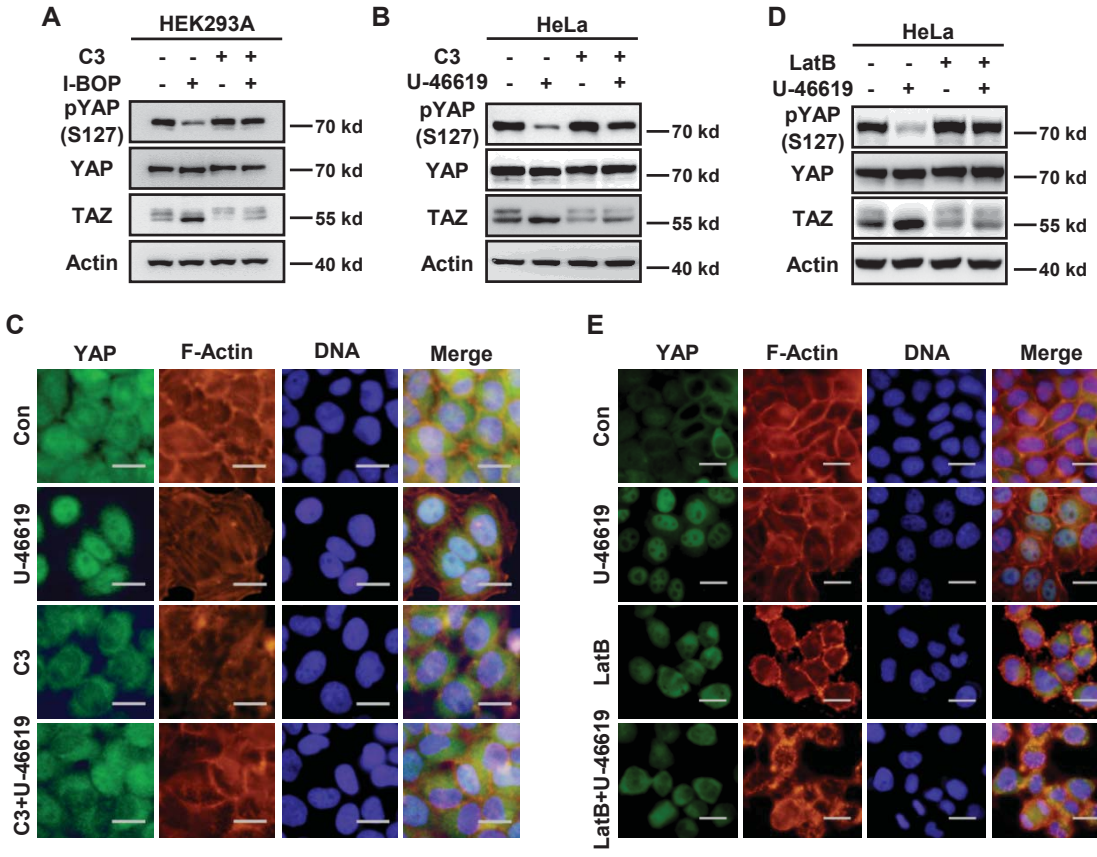

Supplemental Figure 6

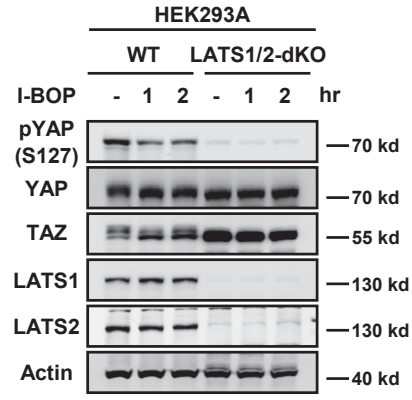

Supplemental Figure 7

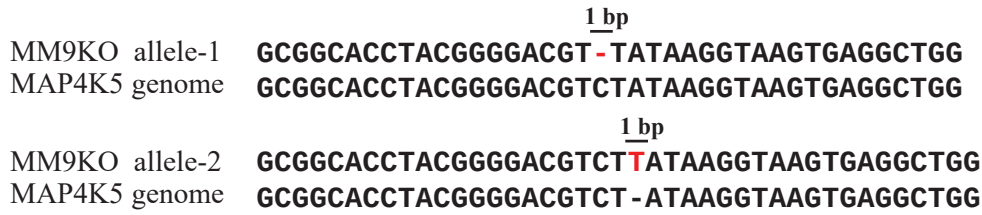

Supplemental Figure 8

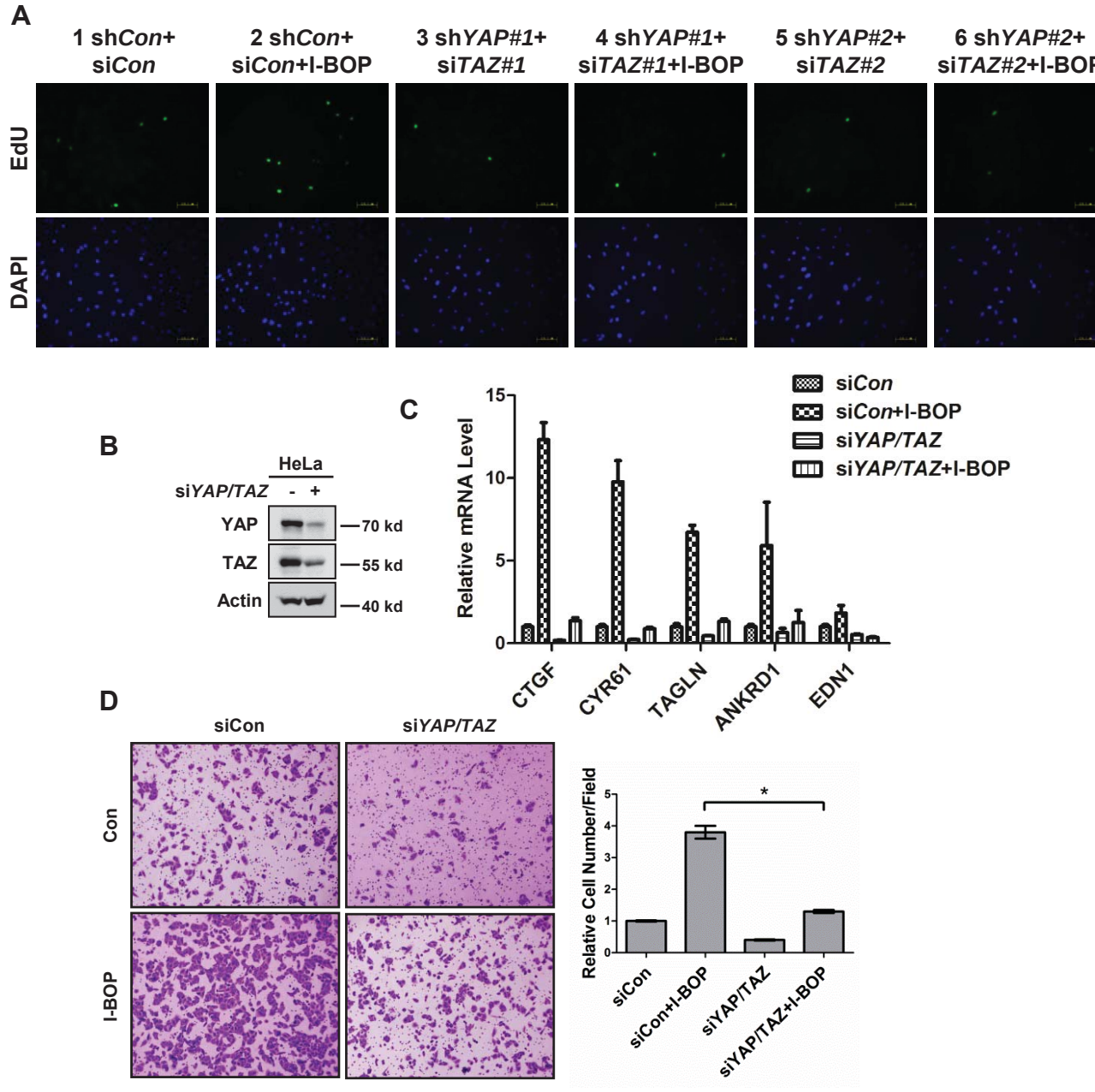

Thromboxane A2 Activates YAP/TAZ to Induce Vascular Smooth Muscle Cell Proliferation and Migration

Xu Feng, Peng Liu, Xin Zhou, Meng-Tian Li, Fu-Long Li, Zhen Wang, Zhi-Peng Meng, Yi-Ping Sun, Ying Yu, Yue Xiong, Hai-Xin Yuan and Kun-Liang Guan

J. Biol. Chem. published online July 5, 2016

Access the most updated version of this article at doi: 10.1074/jbc.M116.739722